DEEP CCD PHOTOMETRY AND VARIABLE STARS IN THE METAL-RICH GLOBULAR CLUSTER M71

PHILIP J. C. HODDER, JAMES M. NEMEC, HARVEY B. RICHER,[1] AND GREGORY G. FAHLMAN[1]
Department of Geophysics and Astronomy, University of British Columbia, 129-2219 Main Mall, Vancouver, British Columbia V6T 1Z4, Canada
Received 26 June 1991; revised 9 October 1991

ABSTRACT

Two sets of observations of the metal-rich globular cluster M71 are presented. The first uses deep CCD exposures to derive a fiducial in V, $B-V$ and compares this with a cluster of similar metallicity, 47 Tuc. Comparison with oxygen enhanced theoretical isochrones leads to age estimates for M71 of from $\sim 14 \pm 2$ Gyr to $\sim 16 \pm 2$ Gyr. Within the limits imposed by the quality of the data, no significant age difference between the two clusters is found. The second set of 73 frames is used to search an overlapping $67'' \times 104''$ area of the cluster for variable stars. Light curves and phase diagrams (where appropriate) are presented for all four of the variables discovered. One variable blue straggler (or SX Phe star) has been identified with a period of $0^{\rm d}050$. Values for its mass depend, of course, on the assumed pulsation mode—$(0.90 \pm 0.47)\mathscr{M}_\odot$ for the first overtone mode, and $(1.57 \pm 0.83)\mathscr{M}_\odot$ for the fundamental mode. One of the variables, with a $0^{\rm d}0582$ period, but with a magnitude $1^{\rm m}75$ below the main sequence turnoff may be a field star. Two candidate eclipsing binary systems were also found. The most likely orbital period of one is $0^{\rm d}372$. This value, and the shape of the light curve, suggest that it could be a W UMa type variable. No period was obtainable for the other candidate binary due to a lack of phase coverage. Further data is needed to confirm and strengthen these claims, and to check for cluster membership.

1. INTRODUCTION

The globular cluster M71 is a small, metal-rich cluster lying close to the galactic plane. Together with 47 Tuc it is one of the brightest and nearest of the "disk" globular clusters and can be studied in some detail. The first major modern work on M71 is that of Arp & Hartwick (1971), conducted using photoelectric and photographic observations. They noted the existence of a small number ($\lesssim 10$) of blue stragglers, and derived estimates for the age, reddening, metallicity, and distance. Cudworth (1985) gives photographic photometry and membership probabilities for stars in the M71 field brighter than $V \approx 16.8$. Richer & Fahlman (1988) identified both a sequence of white dwarf candidates and over 50 blue stragglers using deep CCD photometry of a large $(6' \times 4')$ area of M71. They also derived better estimates of the foreground reddening and distance modulus. A further study (Richer & Fahlman 1989) investigated both the mass and luminosity functions of M71 using the same data. Part of the previously unpublished data gathered for that work is presented here. Heasley & Christian (1991) compare their CCD photometry to the Hesser *et al.* (1987) photometry of 47 Tuc and claim an age difference of ~ 3 Gyr, with M71 being the older cluster.

Zinn (1985) presents convincing evidence for the existence of two populations of globular clusters (halo and intermediate), partly on the examination of the distribution of metallicity. Clusters with an [Fe/H] more metal rich than -0.8 can be identified with this latter population and M71 falls into this category. In support of this Allen & Martos (1988) show, by performing numerical integrations of the cluster's orbit backwards in time, that M71 has a very similar galactic orbit to the open cluster M67. In fact, in plots of metal abundance versus apocentric distance, pericentric distance and orbital eccentricity, M71 always groups with the galactic clusters in their sample rather than with the other globular clusters which tends to strengthen the idea that M71 is a disk population object. However it should be borne in mind that Allen and Martos use the cluster proper motions derived by Cudworth (1985), and that these are uncertain at almost the 50% level.

Sawyer Hogg (1973) catalogues four variable stars in M71, including an eclipsing binary. However Liller & Tokarz (1981) show, on the basis of its radial velocity, that the latter object is probably a field star. Cudworth (1985) notes that two other variables may also be present using data from that study in addition to a study by Welty (private communication to Cudworth) and one by Frogel *et al.* (1979) who cite Sawyer Hogg (private communication to Frogel *et al.*). All these variables lie near the tip of the red giant branch, and none are within the field studied in this survey.

The initial objective of this study, the preliminary results of which have been discussed in Hodder *et al.* (1991), was to search for variable blue stragglers in M71. However, the method employed in the data analysis enabled any type of variable with a period from approximately 30 min to 7 hr to be searched. Section 2 outlines the observations and calibration and Sec. 3 discusses the data analysis procedures. Section 4 presents a deep color–magnitude diagram for M71. Section 5 discusses the variables discovered, while Sec. 6 summarizes the results obtained in this study.

2. OBSERVATIONS AND DATA REDUCTION

2.1 The Deep Data

Richer & Fahlman (1988) presented a search for white dwarfs in M71 using deep CCD photometry of the inner $6' \times 4'$ of the cluster. This was accomplished using U, $U-V$ photometry—the B data was not presented. Here we present the V, $B-V$ photometry of the NE field described in the Richer and Fahlman study. In addition to the deep photom-

[1] Visiting Astronomer, Canada–France–Hawaii Telescope. CFHT is operated by the National Research Council of Canada, the Center National de la Recherche Scientifique of France, and the University of Hawaii.

 0004-6256/92/020460-20$00.90

etry we have included the results from short exposure frames to study the giants and horizontal branch stars.

A more complete description of the data is given in Richer & Fahlman (1988)—a brief summary is given here. The observations were made on 1986 August 2/3 using the double density RCA CCD detector at the prime focus of the 3.6 m Canada–France–Hawaii Telescope. The full width at half maximum (FWHM) of the point spread functions of these frames is typically 0."7, and no frame with a FWHM greater than 0."8 was used in the reductions. The deep V exposure times were 600 s long and the best three frames were averaged together to produce a final frame. The deep B exposures were 900 s long and the best two were averaged. Two short (60 s) exposure frames, one each in V and B, were obtained to study the giant branch. During the whole observing run a total of four fields were observed—the northeast field generally had the best image quality and the photometry from it is presented here. The long exposure and short exposure data were calibrated independently. Standard colors $(B-V)$, were obtained from the instrumental colors $(b-v)$, through an equation of the form

$$(B-V) = \alpha(b-v) + \text{constant}.$$

The color coefficient, determined from equatorial standards, was found to be 1.27, consistent with other photometry done with this chip and filter combination at CFHT. No color term was needed for the V transformation. An unexplained systematic offset was found between the long and short exposure datasets. These mean offsets (calculated from 520 stars) were

$$B_{\rm long} - B_{\rm short} = 0.090 \pm 0.064,$$

$$V_{\rm long} - V_{\rm short} = 0.119 \pm 0.068.$$

The short exposure frames were of noticeably poorer image quality and seeing than the long exposure frames. Consequently magnitudes derived from the short exposure frames had higher photometric errors and were therefore shifted onto the long exposure system. This data set was then used to calibrate the data for the variable star search.

2.2 The Variable Search Data

The CCD frames used in the search for variable stars were taken during the nights 1985 July 11/12 to 14/15 at the 3.6 m Canada–France–Hawaii Telescope by H.B.R. and G.G.F. The RCA1 chip was used at the $f/8$ Cassegrain focus resulting in a plate scale of 0."21 per pixel. A total of 87 frames of approximately the same field of M71 were taken over that period, of which 75 were reduced for this analysis. The remaining 13 were not reduced owing to the poor seeing, and consequently increased crowding, on those images. A log of the observations is given in Table 1. Approximately the same area (67"×104"), centered 30" north and 55" east of the cluster center was observed in each case. This field is almost completely contained in the NE field of the deep photometry. The seeing in the V band on each of the four nights was typically 0."7, 1."0, 0."6, and 0."5, respectively.

After preprocessing each frame was reduced using the DAOPHOT computer program (Stetson 1987) to produce lists of coordinates and magnitudes for each star on the frame. The number of stars measured on each frame ranged from ~1800 on the best frame to ~700 on the worst frame. A list of 20 moderately bright (but unsaturated) and uncrowded stars was compiled to determine the PSF for each frame. Because of variations in seeing and position of each frame, typically a dozen stars from this list were finally used in the determination of each PSF. Positions and magnitudes for each star on the frame were determined by the DAOPHOT profile fitting software packages described in Stetson (1987).

Calibration of the 1985 time series data was achieved using a two step process. First, stars from the calibrated long exposure frames of 1986 were identified in two 1985 reference frames, one in each filter. Stars with an error in B and V in the long exposure frames of more than 0ᵐ02 were excluded, leaving 56 stars for the calibration of the reference frame. Then the offsets between the calibrated reference frame and the other frames in the time series were determined as follows. A list of stars found on *all* time series frames was compiled. For each of these frames the mean magnitude difference between it and the reference frame was calculated using the stars on this list. The mean difference for a given frame was then applied to *all* the measured magnitudes on the appropriate frame thus placing it on the same magnitude scale as the reference frame. The standard deviation of these mean magnitude differences were of the order of 0ᵐ001 to 0ᵐ0001. These errors were added in quadrature to the appropriate magnitudes.

TABLE 1. Condensed observing log.

Date (1)	Time (U.T.) (2)	V frames (3)	B frames (4)	Field (5)
1985 July 12/13	08:34 – 14:37	23	9	Variable search
1985 July 13/14	08:24 – 14:08	2	11	Variable search
1985 July 14/15	05:43 – 14:56	0	2	Variable search
1985 July 15/16	10:11 – 13:58	15	9	Variable search
1986 August 2/3	11:35 – 12:54	3L/1S[a]	2L/1S[b]	Large field exposures

a) Long exposures (L) were 600 s; short exposure (S) 60 s
b) Long exposures were 900 s; short exposure 60 s

3. A DEEP COLOR–MAGNITUDE DIAGRAM

3.1 Photometry

The photometry from both the long and the short exposure frames obtained in 1986 was combined to produce a color–magnitude diagram (CMD) as follows. The final lists of photometry were matched together and compared. If a star appeared on both lists and its V magnitude was brighter than 17.5, the data from the short exposure frames were used, otherwise the data from the long exposure frames were used. The color–magnitude diagram resulting from the final data list is tabulated in Table 2. An attempt was then made to identify stars brighter than $V = 16.85$ with stars from Cudworth's (1985) study. Of the 116 such stars, 77 were identified with a Cudworth star. Of those 42 had a cluster membership probability of 50% or more and are marked with a * in Table 2. The variable stars discussed below are indicated in this table by a number in parentheses to the left of the star number in column (1).

Figure 1 is the color–magnitude diagram of the data in Table 2. In order to reduce the scatter around the giant branch above $V = 16.85$ (Cudworth's magnitude limit) we have only plotted those stars with a 50% (or greater) chance of being cluster members. Below this limit all stars are plotted. Also shown in Fig. 1 is a line marking the position of the horizontal branch at $V_{\rm HB} = 14.44 \pm 0.08$ (the mean V magnitude of the 12 stars in that region of the CMD). From Arp

TABLE 2. Photometry of M71.

ID	X	Y	V	B − V	U − B
1	501.3	647.8	12.18	1.17	1.34
*2	146.6	62.9	12.26	1.85	1.85
*3	77.0	456.7	12.35	1.60	1.79
*4	194.8	670.2	12.46	1.72	1.26
*5	472.6	385.5	12.46	1.58	1.95
*6	482.6	162.1	12.47	1.56	2.01
*7	148.9	517.9	12.48	1.84	1.57
8	152.9	484.5	12.52	1.67	1.91
*9	162.7	46.7	13.11	1.48	1.40
*10	593.7	177.3	13.24	1.26	1.27
*11	106.0	−2.7	13.40	1.51	1.11
*12	487.6	84.7	13.50	1.22	1.08
*13	410.5	33.9	13.58	1.28	0.95
*14	375.6	800.5	13.59	1.23	1.31
*15	132.4	179.0	13.67	1.33	1.17
*16	226.4	111.3	14.25	1.21	1.01
*17	269.5	71.8	14.32	1.01	0.51
*18	625.6	210.6	14.33	1.05	0.63
*19	368.1	108.8	14.35	1.00	0.53
20	136.3	389.3	14.37	0.79	0.29
*21	595.0	380.3	14.37	1.19	0.98
*22	190.8	274.7	14.38	1.06	0.47
*23	278.5	93.7	14.40	1.04	0.52
24	167.2	695.7	14.43	1.27	1.38
*25	170.3	232.5	14.44	1.01	0.44
26	152.2	493.7	14.45	1.02	0.51
27	404.5	657.5	14.47	1.34	1.51
*28	138.4	265.7	14.48	1.10	0.39
*29	447.9	668.0	14.51	0.91	0.52
*30	512.3	45.4	14.52	1.12	0.81
*31	626.1	560.0	14.52	1.07	0.50
*32	262.5	166.5	14.54	0.98	0.52
*33	118.1	617.2	14.55	1.02	0.52
34	244.3	772.6	14.82	1.33	1.48
*35	279.0	114.4	14.83	1.15	0.80
36	45.4	233.8	14.93	1.26	0.67
*37	239.9	623.0	14.94	1.09	0.73
38	103.7	377.1	15.01	1.17	0.68
*39	243.1	178.6	15.09	1.17	0.78
*40	363.6	661.8	15.10	1.04	0.71
41	54.5	235.6	15.16	1.25	0.55
*42	139.8	236.8	15.22	1.18	0.62
43	207.0	727.7	15.25	0.83	0.34
44	96.8	587.2	15.35	1.24	1.21
*45	108.9	168.0	15.36	1.19	0.63
46	375.4	521.4	15.36	1.49	1.55
47	84.8	720.2	15.40	0.78	0.01
48	546.9	326.7	15.40	1.30	1.37
49	480.9	426.0	15.42	1.04	0.63
50	301.1	34.0	15.42	1.39	1.23
51	218.7	141.6	15.47	0.70	0.10
*52	109.2	91.4	15.48	1.12	0.21
*53	566.0	367.6	15.56	1.06	0.63
*54	586.0	363.2	15.59	1.08	0.65
55	402.0	529.9	15.59	1.12	0.60
*56	324.3	458.8	15.67	1.07	0.63
57	57.5	601.1	15.69	1.12	0.60
58	310.7	384.5	15.77	0.97	0.52
59	281.1	29.5	15.77	1.14	0.67
*60	510.5	93.0	15.77	0.87	0.52
61	14.5	498.7	15.81	1.19	0.49
62	630.0	286.7	15.89	0.89	0.44
63	166.9	886.4	15.96	1.35	1.46
64	87.5	269.3	16.00	1.17	0.37
65	140.4	820.3	16.00	1.09	0.58

ID	X	Y	V	B − V	U − B
66	372.1	308.9	16.02	1.15	1.21
67	253.4	339.0	16.08	0.98	0.63
68	107.9	256.8	16.08	1.15	0.50
69	471.8	649.3	16.09	1.23	1.25
*70	31.9	222.8	16.09	0.72	−0.17
71	340.0	99.9	16.11	1.06	0.51
72	529.7	375.6	16.12	0.99	0.53
73	52.6	15.0	16.13	1.59	1.23
74	529.1	766.3	16.18	0.64	0.15
75	221.9	121.2	16.20	1.03	0.55
76	383.3	401.0	16.21	1.00	0.47
77	292.0	19.5	16.23	0.78	−0.04
78	177.0	359.4	16.24	1.06	0.53
79	115.5	254.8	16.25	1.13	0.49
80	399.0	188.1	16.25	0.77	0.31
(1) 81	454.0	137.5	16.25	0.57	−0.21
82	186.6	312.5	16.25	0.86	0.19
*83	264.6	735.6	16.28	0.92	0.49
84	557.8	354.8	16.31	1.02	0.49
85	276.0	237.3	16.32	0.58	0.07
86	75.7	14.4	16.32	1.18	0.51
87	618.9	219.1	16.32	1.03	0.85
88	566.1	522.0	16.40	1.22	0.85
89	181.1	245.1	16.42	0.97	0.29
90	324.2	904.7	16.42	0.73	−0.04
91	149.6	395.6	16.47	1.03	0.47
92	511.5	860.3	16.52	1.20	0.89
93	22.3	393.6	16.52	1.52	1.31
94	107.2	10.4	16.52	1.25	0.35
95	195.0	748.1	16.53	0.97	0.36
96	168.7	180.7	16.60	1.05	0.45
97	487.0	288.1	16.61	0.96	0.50
98	622.3	657.3	16.62	1.28	1.34
99	515.5	150.6	16.63	1.00	0.50
100	221.4	373.5	16.64	0.96	0.47
101	200.6	112.7	16.64	0.97	0.37
*102	373.9	225.4	16.64	0.87	0.28
*103	193.9	414.0	16.67	0.98	0.48
104	213.5	708.0	16.68	0.95	0.52
105	16.4	340.5	16.69	0.77	−0.12
106	189.1	164.8	16.69	0.63	−0.06
107	633.0	514.3	16.70	0.66	−0.07
108	59.2	43.7	16.72	0.86	−0.21
109	232.4	293.4	16.73	0.88	0.19
110	84.5	221.6	16.75	1.10	0.43
111	45.7	28.5	16.76	1.05	0.24
112	145.3	74.3	16.77	1.34	0.47
113	202.6	591.1	16.82	1.02	0.43
114	93.0	64.1	16.83	0.79	−0.17
115	76.9	52.9	16.84	1.14	0.20
116	89.7	381.0	16.86	1.10	0.48
117	498.3	155.1	16.91	0.93	0.56
118	111.2	831.7	16.91	0.92	0.16
119	312.3	645.7	16.91	0.64	0.09
120	421.4	699.2	16.92	0.65	0.22
121	593.7	116.4	16.93	0.90	0.28
122	569.5	94.1	16.93	0.90	0.23
123	254.5	321.1	16.94	0.99	0.40
124	345.3	279.7	16.95	0.66	0.17
125	122.4	837.9	16.96	0.85	0.13
126	145.0	28.9	16.96	1.24	0.38
127	48.4	216.5	16.96	0.99	0.76
128	30.3	74.3	16.97	0.90	−0.13
129	387.2	413.1	16.98	0.99	0.49
130	310.9	53.0	16.98	0.87	0.02

ID	X	Y	V	B − V	U − B
131	122.4	−3.3	16.98	1.16	−0.12
132	229.0	172.0	16.98	1.00	0.50
133	402.7	60.2	16.98	1.07	0.53
134	211.5	712.7	16.98	0.76	0.25
135	14.8	775.7	17.03	1.25	0.33
136	165.3	57.8	17.03	1.01	0.23
137	453.4	655.2	17.04	0.93	0.51
138	626.1	443.2	17.05	1.07	0.58
139	158.7	34.9	17.06	0.97	0.08
140	228.6	431.0	17.09	0.90	0.44
141	451.1	193.2	17.11	0.96	0.40
142	321.0	517.0	17.11	1.05	0.41
143	541.1	162.0	17.11	0.94	0.67
144	604.2	666.4	17.13	1.19	1.10
145	215.4	187.5	17.13	0.98	0.41
146	377.0	18.1	17.14	0.58	0.79
147	489.6	369.4	17.15	0.96	0.44
148	353.9	29.1	17.17	1.03	0.30
149	22.7	190.9	17.17	1.11	0.51
150	308.8	673.2	17.22	0.50	−0.05
151	577.4	323.9	17.27	0.99	0.51
152	556.1	779.6	17.28	0.90	0.33
153	99.4	48.3	17.29	0.89	−0.23
154	320.8	503.4	17.29	0.76	−0.05
155	202.8	78.0	17.29	1.07	0.40
156	230.0	82.1	17.31	0.70	−0.06
157	213.5	82.7	17.32	0.90	0.02
158	485.6	193.2	17.32	1.10	0.82
159	253.0	761.8	17.33	0.94	0.43
160	63.7	163.3	17.33	0.75	0.59
161	278.5	756.3	17.35	0.65	0.15
162	153.0	117.0	17.35	0.81	−0.12
163	51.8	146.8	17.35	1.08	0.16
164	453.9	717.7	17.36	1.09	1.05
165	478.6	836.0	17.36	0.68	−0.09
166	320.5	239.7	17.37	0.76	0.32
167	192.8	224.3	17.39	0.96	0.26
168	216.8	434.7	17.40	0.91	0.38
169	412.5	228.5	17.41	0.84	0.01
170	511.4	8.6	17.41	1.04	0.26
171	401.2	175.2	17.41	0.82	0.16
172	536.4	34.5	17.42	0.72	−0.04
173	288.7	280.9	17.43	0.83	0.44
174	63.5	163.3	17.44	0.92	0.39
175	189.9	463.9	17.44	0.85	0.05
176	478.9	894.8	17.44	0.81	0.04
177	76.2	247.6	17.45	0.91	0.02
178	189.9	464.1	17.46	0.81	0.08
179	361.3	197.5	17.48	0.99	0.71
180	532.3	359.1	17.48	0.90	0.36
181	49.5	20.5	17.48	0.97	0.16
182	524.6	418.6	17.49	0.92	0.29
183	354.2	242.0	17.49	0.81	0.31
184	304.6	396.6	17.50	0.92	0.25
185	360.0	496.8	17.50	0.82	0.11
186	139.0	503.1	17.51	0.95	0.05
187	247.2	247.1	17.51	0.85	0.20
188	273.8	631.9	17.52	0.90	0.19
189	255.2	306.0	17.52	0.87	0.26
190	51.6	147.1	17.52	0.88	0.41
191	196.9	190.3	17.52	0.94	0.26
192	511.6	213.1	17.52	0.88	0.19
193	461.8	159.1	17.53	0.91	0.28
194	226.6	9.9	17.53	0.63	−0.08
195	514.0	373.9	17.53	0.84	0.10

TABLE 2. (continued)

ID	X	Y	V	B − V	U − B	ID	X	Y	V	B − V	U − B	ID	X	Y	V	B − V	U − B
196	479.1	372.5	17.53	0.82	0.14	261	462.5	215.8	17.66	0.81	0.03	326	159.4	432.1	17.79	0.84	0.06
197	126.8	75.4	17.54	0.83	0.06	262	226.6	45.0	17.66	0.92	0.05	327	70.4	−3.2	17.80	1.23	−0.22
198	42.2	89.3	17.54	0.74	0.44	263	176.2	461.7	17.67	0.88	0.09	328	496.7	328.1	17.80	1.22	0.85
199	349.1	158.7	17.54	0.81	0.14	264	108.2	587.2	17.67	0.81	0.14	329	350.0	346.2	17.80	0.76	0.00
200	233.9	809.7	17.56	0.88	0.22	265	85.0	424.6	17.67	0.82	0.16	330	369.0	117.8	17.81	0.80	0.06
201	298.2	67.9	17.56	0.89	0.25	266	219.6	159.4	17.67	0.81	0.04	331	348.7	109.7	17.81	0.78	0.07
202	120.3	781.5	17.56	0.81	0.28	267	304.7	28.0	17.67	0.72	0.19	332	236.0	860.6	17.81	0.81	0.03
203	176.6	221.5	17.57	0.66	−0.02	268	123.5	666.3	17.67	0.82	0.06	(4) 333	416.5	202.8	17.81	0.49	−0.33
204	38.6	7.6	17.57	0.85	0.40	269	105.4	135.4	17.67	0.75	0.08	334	391.3	90.8	17.82	1.47	1.40
205	23.1	8.4	17.57	0.73	0.03	270	57.6	507.5	17.68	0.81	0.13	335	233.2	519.1	17.82	0.82	0.10
206	424.2	822.2	17.57	0.92	0.35	271	601.8	129.3	17.68	0.79	0.04	336	436.3	355.5	17.82	1.00	0.70
207	188.0	353.2	17.57	0.67	−0.03	272	233.5	123.4	17.68	0.78	0.07	337	167.0	267.8	17.82	0.79	0.05
208	304.5	214.7	17.58	0.87	0.25	273	104.5	629.3	17.68	0.81	0.11	338	226.9	45.0	17.82	0.74	0.08
209	70.6	543.8	17.58	0.87	0.18	274	356.1	793.0	17.68	0.73	0.26	339	468.8	260.5	17.83	0.79	0.05
210	276.8	172.0	17.58	0.85	0.23	275	370.1	439.9	17.69	0.95	0.57	340	8.3	53.5	17.83	0.70	0.77
211	530.9	93.4	17.58	0.85	0.27	276	339.7	716.5	17.69	0.80	0.02	341	10.4	88.2	17.83	0.79	0.28
212	414.6	781.0	17.58	0.84	0.52	277	232.7	368.2	17.69	1.25	1.19	342	144.0	29.8	17.83	0.05	0.42
213	607.6	81.7	17.59	0.81	0.10	278	543.8	377.8	17.69	0.79	0.08	343	69.3	251.8	17.83	0.80	0.06
214	264.2	83.6	17.59	0.78	0.08	279	505.4	258.8	17.69	0.79	0.03	344	118.7	448.4	17.83	0.80	0.05
215	150.7	417.3	17.59	0.91	0.13	280	633.5	151.8	17.69	0.81	0.06	345	140.3	94.6	17.84	0.77	0.12
216	256.4	803.9	17.59	0.81	0.13	281	129.7	851.6	17.70	0.82	0.08	346	449.9	130.4	17.84	0.75	0.11
217	81.1	476.2	17.59	0.92	0.09	282	313.4	119.7	17.70	0.79	0.03	347	197.3	522.6	17.84	0.81	0.08
218	620.7	218.0	17.59	−0.55	0.78	283	322.8	205.0	17.71	0.93	0.27	348	456.6	225.2	17.84	0.77	0.00
219	272.1	588.5	17.60	0.94	0.35	284	126.8	381.7	17.71	0.84	0.02	349	126.8	381.7	17.85	0.70	0.09
220	235.6	208.5	17.60	0.67	−0.07	285	529.5	120.7	17.71	0.80	0.05	350	316.6	418.6	17.85	0.78	0.07
221	355.0	455.1	17.60	0.82	0.17	286	314.6	331.6	17.71	0.77	0.03	351	112.5	683.5	17.85	0.81	0.12
222	568.9	324.2	17.60	0.92	0.22	287	366.2	766.4	17.72	0.77	0.04	352	59.6	77.4	17.85	0.75	0.09
223	618.8	117.5	17.60	0.78	0.07	288	294.4	263.9	17.72	0.79	0.04	353	132.1	85.7	17.85	0.77	0.05
224	378.2	652.6	17.60	0.88	0.16	289	43.2	347.4	17.72	0.78	0.25	354	256.5	100.9	17.86	0.84	0.14
225	473.2	83.5	17.60	0.75	0.08	290	143.8	98.1	17.72	0.95	−0.09	355	188.7	26.0	17.86	0.75	0.13
226	77.2	192.6	17.60	0.82	0.14	291	198.8	126.9	17.73	0.81	0.09	356	613.5	280.2	17.86	0.74	0.06
227	35.7	60.6	17.61	0.85	0.10	292	559.9	107.8	17.73	0.72	0.05	357	224.3	26.6	17.86	0.76	0.01
228	120.7	36.7	17.61	0.84	0.15	293	325.8	210.9	17.73	0.73	0.20	358	136.7	224.9	17.87	0.81	0.12
229	48.7	254.4	17.61	0.89	0.22	294	322.7	204.8	17.73	0.80	0.33	359	567.4	87.0	17.87	0.83	0.08
230	229.6	553.3	17.61	0.89	0.24	295	91.3	279.8	17.73	0.81	0.19	360	236.0	328.1	17.88	0.78	0.03
231	76.1	248.2	17.61	0.73	0.43	296	154.8	90.5	17.74	0.76	0.07	361	317.0	139.8	17.88	0.80	0.06
232	34.1	330.2	17.61	0.76	0.12	297	49.5	219.8	17.74	0.80	0.03	362	302.2	678.8	17.88	0.79	0.02
233	472.1	688.4	17.61	0.80	0.05	298	308.2	947.0	17.74	0.88	−0.02	363	193.6	137.2	17.88	0.81	0.04
234	212.7	82.6	17.61	0.67	−0.22	299	131.0	26.1	17.74	0.75	−0.04	364	376.2	323.0	17.88	0.85	0.30
235	575.3	101.1	17.62	0.81	0.03	300	194.8	25.5	17.74	0.63	0.20	365	472.0	253.6	17.88	0.77	0.01
236	287.8	355.1	17.62	0.83	0.25	301	154.9	231.9	17.75	0.73	0.21	366	582.6	432.4	17.89	0.78	0.06
237	74.4	152.6	17.62	0.84	0.23	302	523.3	311.5	17.75	0.80	0.08	367	20.6	13.2	17.89	0.88	−0.01
238	100.4	75.2	17.62	0.70	0.12	303	499.1	560.6	17.75	0.76	0.12	368	515.0	142.0	17.89	0.81	0.05
239	175.9	319.1	17.62	0.81	0.12	304	8.1	40.9	17.75	0.99	−0.09	369	422.5	860.6	17.89	0.80	−0.02
240	138.8	503.3	17.62	0.85	0.18	305	124.0	45.4	17.76	0.79	0.06	370	285.6	345.8	17.89	0.78	0.03
241	216.7	993.8	17.63	0.87	0.07	306	422.2	370.2	17.76	0.77	0.05	371	37.5	120.5	17.89	0.70	0.13
242	250.3	142.0	17.63	0.82	0.08	307	557.2	489.6	17.76	0.79	0.07	372	186.2	193.2	17.89	0.78	0.02
243	206.0	40.1	17.63	0.87	0.19	308	167.1	267.7	17.76	0.88	−0.09	373	203.3	198.4	17.89	0.74	0.12
244	281.9	174.6	17.63	0.86	0.12	309	409.3	77.7	17.76	0.79	0.08	374	248.9	147.5	17.90	0.80	0.01
245	177.4	11.2	17.63	0.89	0.27	310	172.1	148.6	17.77	0.81	0.04	375	514.2	165.0	17.90	0.74	0.07
246	323.5	339.8	17.64	0.74	0.06	311	52.4	248.5	17.77	0.79	0.10	376	432.5	397.2	17.90	0.75	0.03
247	193.3	695.2	17.64	0.81	0.17	312	553.8	197.9	17.77	0.79	0.05	377	160.4	159.9	17.90	0.81	0.00
248	108.3	587.1	17.64	0.86	0.05	313	133.7	309.1	17.77	0.79	0.12	378	394.3	580.1	17.90	0.86	0.28
249	257.6	523.0	17.64	0.84	0.22	314	608.3	718.2	17.77	0.71	0.11	379	169.6	159.5	17.90	0.78	−0.00
250	139.1	670.0	17.65	0.83	0.06	315	260.8	−1.1	17.78	0.85	−0.09	380	113.9	349.6	17.91	0.64	0.10
251	25.3	42.8	17.65	0.88	0.11	316	254.6	443.5	17.78	0.80	0.10	381	498.3	274.4	17.91	0.79	0.02
252	37.6	266.9	17.65	0.81	0.13	317	426.8	430.5	17.78	0.79	0.30	382	193.7	182.1	17.91	0.79	0.00
253	164.4	94.7	17.65	0.85	0.07	318	415.9	303.4	17.79	0.78	0.04	383	193.8	137.0	17.91	0.78	0.10
254	36.3	67.9	17.65	0.83	0.08	319	251.2	453.3	17.79	0.82	0.09	384	173.2	201.9	17.92	0.79	0.02
255	390.4	306.1	17.65	0.77	0.07	320	50.4	133.6	17.79	0.76	0.02	385	492.4	188.4	17.92	0.78	0.05
256	350.5	45.7	17.65	0.77	0.22	321	302.3	287.7	17.79	0.75	0.09	386	394.4	580.0	17.92	0.89	0.25
257	90.1	199.2	17.65	0.81	0.07	322	66.9	160.6	17.79	0.77	0.04	387	442.3	154.1	17.93	0.77	0.05
258	72.5	833.1	17.66	0.86	0.23	323	470.3	829.0	17.79	0.81	−0.03	388	378.0	376.8	17.93	0.79	0.01
259	557.9	316.0	17.66	0.82	0.11	324	363.2	525.9	17.79	0.79	0.15	389	459.8	270.5	17.93	0.77	0.04
260	472.3	557.3	17.66	0.79	0.15	325	225.0	3.3	17.79	0.75	0.07	390	572.7	170.6	17.93	0.77	0.01

TABLE 2. (continued)

ID	X	Y	V	B − V	U − B
391	495.4	350.0	17.94	0.81	0.04
392	209.6	461.9	17.94	0.80	0.05
393	412.7	590.6	17.94	0.81	0.11
394	66.0	745.8	17.94	0.83	0.09
395	382.5	378.1	17.94	0.79	0.05
396	390.0	14.5	17.95	0.78	0.07
397	532.0	217.9	17.95	0.76	−0.01
398	113.1	867.7	17.95	1.13	0.93
399	77.8	492.9	17.95	0.85	−0.01
400	258.9	443.2	17.95	0.79	0.07
401	98.7	107.4	17.95	0.73	0.12
402	136.6	418.4	17.95	0.79	0.07
403	181.2	340.5	17.95	0.76	0.05
404	284.0	170.9	17.95	0.80	0.05
405	495.5	350.1	17.95	0.78	0.03
406	63.0	749.0	17.95	0.88	−0.01
407	236.4	643.0	17.96	0.89	0.49
408	378.2	376.6	17.96	0.75	0.01
409	412.8	538.2	17.96	1.06	0.72
410	357.5	56.5	17.96	0.76	0.11
411	159.1	193.7	17.97	0.77	0.16
412	240.5	369.6	17.97	0.78	0.08
413	591.6	16.3	17.98	0.75	0.01
414	450.4	106.7	17.98	0.77	0.05
415	256.1	101.1	17.98	0.65	0.11
416	309.1	448.7	17.98	0.79	0.05
417	117.4	48.6	17.98	0.77	0.04
418	117.5	194.1	17.98	0.79	0.04
419	310.0	432.2	17.98	1.17	1.08
420	183.2	41.5	17.98	0.78	0.10
421	631.5	117.9	17.98	0.77	0.06
422	216.8	47.3	17.99	0.78	0.03
423	167.6	172.2	17.99	0.83	0.00
424	280.1	935.0	17.99	0.82	0.00
425	62.9	749.0	18.00	0.84	0.14
426	333.6	592.2	18.00	0.79	0.08
427	375.7	431.5	18.00	0.75	0.03
428	503.2	84.3	18.01	0.79	0.17
429	53.7	357.1	18.01	0.76	0.11
430	370.3	63.0	18.02	0.80	0.04
431	397.0	658.9	18.02	0.53	0.46
432	113.3	361.0	18.02	0.77	0.07
433	56.5	637.5	18.02	0.92	0.38
434	276.7	−3.3	18.02	0.85	0.25
435	610.9	157.9	18.03	0.82	0.03
436	551.1	457.3	18.03	1.02	0.70
437	473.3	920.4	18.03	0.80	3.12
438	213.0	358.6	18.04	0.79	0.09
439	437.6	532.3	18.05	0.77	0.08
440	189.4	0.7	18.05	0.98	−0.19
441	283.8	781.4	18.05	0.89	0.41
442	234.5	104.3	18.05	0.75	0.16
443	300.6	628.7	18.06	0.79	0.07
444	252.5	5.2	18.06	0.90	0.08
445	386.0	182.1	18.06	0.81	0.05
446	119.9	81.4	18.06	0.81	0.10
447	598.8	11.7	18.07	0.78	0.16
448	115.3	110.2	18.07	0.70	0.13
449	415.2	136.2	18.08	0.80	0.02
450	533.2	535.2	18.08	0.81	−0.06
451	484.1	208.9	18.08	0.74	0.23
452	452.7	432.6	18.08	0.76	0.07
453	533.1	535.2	18.09	0.75	0.06
454	258.5	188.5	18.09	0.80	0.02
455	252.4	5.2	18.09	0.81	0.07

ID	X	Y	V	B − V	U − B
456	245.2	38.8	18.09	0.80	0.00
457	170.2	262.7	18.09	0.92	0.14
458	363.0	229.9	18.09	0.77	0.03
459	347.8	273.4	18.09	0.83	0.02
460	375.3	431.4	18.09	0.71	0.11
461	507.0	289.2	18.10	0.88	0.41
462	507.1	289.0	18.10	0.88	0.44
463	533.1	312.0	18.11	0.78	0.03
464	39.1	674.5	18.11	0.86	0.04
465	129.4	409.2	18.11	0.86	0.24
466	191.9	232.6	18.11	0.91	0.06
467	500.3	169.9	18.11	0.78	0.08
468	79.6	597.9	18.11	0.79	0.05
469	450.5	107.1	18.11	0.78	0.02
470	9.1	13.9	18.11	0.75	0.39
471	144.3	253.6	18.11	0.75	0.09
472	221.2	319.2	18.12	0.79	0.07
473	516.8	539.2	18.12	0.76	0.05
474	453.7	771.3	18.12	0.66	−0.02
475	77.4	419.1	18.12	0.88	−0.06
476	425.6	817.1	18.13	0.73	−0.02
477	262.6	2.8	18.13	0.86	−0.10
478	90.2	91.1	18.13	0.67	−0.07
479	408.0	623.4	18.14	0.79	0.05
480	438.1	100.7	18.14	0.71	−0.06
481	192.4	402.5	18.14	0.78	0.03
482	399.0	670.8	18.14	0.89	0.40
483	27.1	57.5	18.14	0.71	0.20
484	160.4	27.7	18.14	0.77	0.21
485	516.3	279.5	18.14	0.80	0.02
486	161.4	332.4	18.15	0.77	0.07
487	451.0	545.4	18.15	0.84	−0.01
488	308.5	872.4	18.15	0.79	−0.04
489	98.2	391.0	18.15	0.80	0.17
490	116.5	578.7	18.16	0.79	0.08
491	98.1	204.4	18.16	0.84	0.08
492	21.3	13.7	18.16	0.60	0.09
493	319.4	329.4	18.16	0.77	0.03
494	140.2	315.8	18.16	0.78	0.07
495	403.9	357.5	18.16	0.74	0.20
496	335.4	206.1	18.17	0.78	0.04
497	289.9	205.3	18.17	0.80	0.05
498	264.5	497.7	18.17	0.84	0.13
499	41.7	407.6	18.18	0.79	0.12
500	140.3	315.7	18.18	0.84	−0.05
501	181.6	564.9	18.18	0.80	0.08
502	30.5	36.9	18.18	0.78	−0.03
503	170.1	262.7	18.18	0.82	0.12
504	52.1	932.2	18.18	0.82	0.20
505	451.0	545.6	18.18	0.78	0.05
506	340.2	238.8	18.18	0.77	0.05
507	478.0	637.5	18.18	0.78	0.21
508	269.1	2.4	18.19	0.75	0.05
509	464.0	236.6	18.19	0.94	0.36
510	338.4	198.5	18.19	0.80	0.03
511	288.2	74.5	18.19	0.82	0.05
512	399.9	340.5	18.19	0.77	0.03
513	126.8	217.0	18.19	0.88	0.12
514	583.8	467.6	18.19	0.79	0.08
515	75.5	861.3	18.20	1.23	1.17
516	8.7	231.2	18.20	1.03	0.69
517	112.1	389.1	18.20	0.76	0.10
518	97.9	204.5	18.20	0.77	0.09
519	12.0	126.3	18.21	0.70	0.08
520	316.1	103.9	18.21	0.53	0.15

ID	X	Y	V	B − V	U − B
521	120.0	147.2	18.21	0.81	0.13
522	395.5	86.8	18.21	0.83	0.14
523	527.5	211.3	18.22	0.78	0.03
524	332.5	548.1	18.22	0.79	0.12
525	225.2	797.7	18.23	0.79	0.03
526	213.6	114.6	18.23	0.88	0.07
527	25.5	93.8	18.23	0.71	0.77
528	120.8	113.1	18.23	0.79	0.10
529	395.7	729.5	18.23	0.75	−0.01
530	570.4	79.9	18.23	0.80	0.04
531	603.1	625.0	18.23	0.89	0.10
532	193.0	526.8	18.23	0.83	0.12
533	155.8	701.3	18.24	0.80	0.09
534	193.2	530.8	18.24	0.81	0.10
535	570.8	424.3	18.24	0.91	0.47
536	483.1	114.9	18.24	0.75	0.11
537	527.7	211.1	18.25	0.80	0.05
538	162.9	183.6	18.25	0.93	0.04
539	427.1	470.0	18.25	0.76	0.14
540	218.9	27.8	18.26	0.84	0.14
541	30.0	799.3	18.26	0.79	0.12
542	454.2	19.1	18.26	0.80	0.04
543	225.7	952.1	18.26	1.05	0.50
544	173.9	65.6	18.26	0.73	0.09
545	251.2	53.8	18.27	0.78	0.04
546	424.8	356.5	18.27	0.77	0.03
547	124.5	97.6	18.27	0.79	0.03
548	228.2	417.5	18.27	0.80	0.08
549	49.8	400.5	18.27	0.79	0.12
550	199.1	383.8	18.27	0.79	0.06
551	245.4	104.2	18.28	0.79	0.07
552	50.7	154.2	18.28	0.75	0.74
553	84.2	24.5	18.28	0.77	−0.04
554	80.0	32.7	18.28	0.76	0.24
555	563.4	391.1	18.28	0.83	0.28
556	80.0	155.3	18.28	0.75	0.04
557	213.4	114.8	18.28	0.74	0.10
558	51.9	81.3	18.28	0.75	0.15
559	110.2	36.3	18.28	1.10	−0.21
560	205.2	679.8	18.29	0.87	0.33
561	34.8	564.9	18.29	0.82	0.10
562	289.1	641.5	18.29	0.86	0.16
563	167.5	652.8	18.30	0.80	0.09
564	285.7	41.3	18.30	0.98	0.64
565	212.1	806.7	18.30	0.84	0.17
566	94.0	377.2	18.30	0.74	0.29
567	96.8	18.2	18.30	0.73	0.08
568	144.3	591.9	18.30	0.97	0.57
569	171.8	110.2	18.30	0.85	0.24
570	444.1	531.9	18.30	0.85	0.32
571	510.9	193.2	18.31	0.78	0.04
572	178.1	113.2	18.31	0.80	0.02
573	469.4	21.5	18.31	0.79	0.05
574	317.9	117.0	18.31	0.79	0.07
575	407.8	496.4	18.31	0.78	0.08
576	372.8	183.0	18.31	0.88	0.20
577	419.9	328.5	18.31	0.76	0.04
578	290.4	153.3	18.31	0.81	0.02
579	319.5	254.2	18.32	0.78	0.14
580	91.7	297.5	18.32	0.78	0.08
581	110.1	36.3	18.32	0.76	−0.01
582	389.1	56.5	18.32	0.78	0.06
583	307.8	207.2	18.32	0.81	0.03
584	322.3	305.2	18.33	0.75	0.05
585	136.0	508.9	18.33	1.02	0.65

TABLE 2. (continued)

ID	X	Y	V	B − V	U − B	ID	X	Y	V	B − V	U − B	ID	X	Y	V	B − V	U − B
586	170.8	78.6	18.33	0.81	0.08	651	139.8	200.7	18.46	0.85	0.04	716	97.9	223.9	18.57	0.87	0.04
587	318.2	116.9	18.33	0.79	0.00	652	100.0	303.7	18.46	0.81	0.15	717	20.5	103.9	18.58	0.64	0.39
588	347.8	385.9	18.33	0.79	0.03	653	127.5	33.2	18.46	0.88	0.21	718	430.3	74.0	18.58	0.80	0.08
589	59.9	90.2	18.33	0.78	0.00	654	127.8	70.6	18.46	0.95	0.27	719	216.8	705.1	18.58	0.87	0.08
590	392.4	546.6	18.33	0.79	0.15	655	386.8	528.5	18.47	0.77	0.20	720	254.6	21.2	18.58	0.87	0.19
591	186.7	204.5	18.34	0.73	0.01	656	465.6	243.2	18.47	0.96	0.49	721	268.6	34.1	18.58	0.89	0.32
592	82.6	391.8	18.34	0.81	0.13	657	154.9	155.8	18.47	0.89	0.12	722	26.1	343.6	18.58	0.75	0.49
593	449.5	87.5	18.35	0.76	0.09	658	172.2	110.1	18.47	0.80	0.03	723	326.7	718.4	18.59	0.80	0.11
594	51.8	280.2	18.35	0.76	0.07	659	420.6	399.1	18.47	0.80	0.06	724	340.5	690.2	18.59	0.80	0.06
595	464.0	98.2	18.35	0.79	0.03	660	341.1	616.2	18.48	0.81	0.06	725	98.1	223.6	18.59	0.90	−0.11
596	80.0	303.3	18.35	0.78	0.20	661	515.5	555.0	18.48	0.80	0.13	726	349.1	25.2	18.59	0.73	0.15
597	86.4	103.1	18.35	0.71	−0.01	662	283.2	136.2	18.48	0.74	0.28	727	228.8	423.3	18.60	0.84	0.07
598	378.7	250.4	18.35	0.78	0.04	663	291.0	315.4	18.48	0.81	0.03	728	62.9	149.7	18.60	0.74	0.12
599	510.0	238.3	18.36	0.78	0.02	664	123.2	237.1	18.48	0.77	0.10	729	534.0	249.4	18.60	0.82	0.07
600	382.9	357.1	18.36	0.78	0.04	665	517.3	422.4	18.49	0.83	0.23	730	286.3	323.9	18.60	0.81	0.09
601	411.6	728.0	18.36	0.77	0.01	666	358.1	45.8	18.49	0.78	0.09	731	587.5	459.4	18.60	0.81	0.14
602	348.0	198.3	18.36	0.79	0.07	667	400.9	453.0	18.49	0.82	0.12	732	394.7	95.4	18.60	0.84	0.14
603	36.7	48.0	18.36	0.99	0.63	668	145.7	283.5	18.49	0.78	0.11	733	394.3	599.5	18.60	0.82	0.12
604	326.3	36.6	18.37	0.80	0.07	669	217.6	386.5	18.49	0.80	0.11	734	203.4	33.5	18.61	0.81	0.07
605	198.4	481.2	18.37	0.95	0.23	670	54.2	181.3	18.49	0.79	0.12	735	516.4	477.1	18.61	0.83	0.15
606	274.0	214.4	18.38	0.79	0.05	671	127.7	37.0	18.50	0.91	0.06	736	81.7	103.4	18.61	0.41	0.13
607	324.0	71.7	18.38	0.86	0.11	672	164.8	640.0	18.50	0.84	0.07	737	113.7	1003.0	18.62	0.84	0.06
608	65.7	908.0	18.38	0.81	0.07	673	92.8	6.2	18.51	0.76	0.17	738	305.5	187.4	18.62	0.86	0.16
609	290.6	56.9	18.38	0.76	0.10	674	105.5	331.3	18.51	1.53	1.39	739	403.4	105.9	18.62	0.83	0.10
610	250.1	810.3	18.38	0.92	0.39	675	42.6	442.9	18.51	0.88	0.15	740	496.3	101.1	18.62	0.83	0.20
611	383.1	356.9	18.38	0.82	0.02	676	256.5	139.4	18.51	0.83	0.04	741	432.7	481.3	18.62	0.81	0.16
612	577.0	559.1	18.38	0.78	0.10	677	45.6	250.4	18.51	0.76	0.16	742	80.2	209.4	18.63	0.79	0.13
613	361.6	259.5	18.39	0.78	0.04	678	476.3	607.7	18.51	1.03	0.74	743	268.5	58.1	18.63	0.77	0.21
614	436.2	615.4	18.39	0.81	0.06	679	624.7	408.6	18.52	0.81	0.09	744	12.9	365.6	18.63	0.78	0.12
615	91.4	797.0	18.39	0.92	0.42	680	424.9	29.1	18.52	0.79	0.12	745	569.0	484.1	18.64	0.82	0.12
616	125.2	465.5	18.39	0.81	0.08	681	333.8	15.2	18.52	0.81	0.13	746	62.9	876.9	18.64	0.90	0.24
617	251.3	164.8	18.39	0.73	0.15	682	141.6	18.0	18.52	0.86	0.18	747	219.8	172.3	18.64	0.82	0.09
618	343.8	27.5	18.39	0.34	−0.03	683	180.2	532.4	18.52	0.89	0.51	748	217.9	70.8	18.64	0.88	0.29
619	54.9	792.4	18.40	0.81	0.08	684	445.7	246.1	18.52	0.88	−0.02	749	515.6	71.9	18.64	0.83	0.08
620	133.2	703.4	18.40	0.91	0.18	685	373.1	125.9	18.52	0.78	0.11	750	448.7	103.4	18.64	0.83	0.09
621	253.5	530.8	18.40	0.84	0.13	686	86.4	33.9	18.53	0.41	0.02	751	459.9	39.6	18.65	0.63	0.06
622	379.4	109.0	18.40	0.72	0.17	687	171.8	119.8	18.53	0.82	0.09	752	242.9	120.4	18.65	0.83	0.08
623	366.6	211.3	18.40	0.92	0.41	688	140.4	491.4	18.53	0.89	1.23	753	480.2	359.4	18.65	0.87	0.14
624	578.7	57.3	18.40	0.78	0.14	689	117.5	73.5	18.53	0.85	0.23	754	525.1	240.4	18.65	0.82	0.05
625	537.0	122.0	18.40	0.81	0.05	690	336.3	390.2	18.53	0.99	0.25	755	397.7	847.7	18.65	1.02	0.11
626	512.1	66.2	18.40	1.12	0.94	691	15.2	959.2	18.53	0.82	0.06	756	594.7	315.2	18.65	0.84	0.11
627	505.9	163.0	18.41	0.78	0.12	692	33.1	54.5	18.53	0.79	0.03	757	190.6	233.1	18.66	0.23	0.59
628	224.1	863.3	18.41	1.01	0.64	693	550.7	630.0	18.53	0.80	0.10	758	289.4	307.0	18.66	0.90	0.39
629	116.3	849.8	18.42	0.90	0.36	694	445.7	246.4	18.54	0.80	0.03	759	517.4	83.5	18.66	0.91	0.57
630	153.4	150.0	18.42	0.81	0.05	695	81.4	610.0	18.54	0.83	0.14	760	176.1	18.6	18.66	0.94	0.11
631	436.4	615.3	18.42	0.74	0.09	696	338.9	769.0	18.54	0.84	0.09	761	236.4	219.6	18.67	0.82	0.08
632	391.1	191.3	18.43	1.00	1.08	697	244.1	801.6	18.54	0.79	0.03	762	328.3	192.6	18.67	0.83	0.06
633	89.3	144.8	18.43	0.78	0.03	698	229.5	699.2	18.54	0.83	0.15	763	293.7	165.6	18.67	0.82	0.13
634	376.1	69.7	18.43	0.81	0.07	699	235.7	9.2	18.55	0.81	0.07	764	478.2	472.9	18.67	0.84	0.11
635	552.6	347.4	18.43	0.81	0.08	700	238.9	398.6	18.55	0.77	0.11	765	185.4	682.6	18.67	1.13	0.47
636	73.7	223.9	18.43	0.83	0.11	701	18.6	767.1	18.55	0.90	0.26	766	618.7	166.6	18.67	1.40	1.38
637	520.3	319.5	18.43	0.77	0.08	702	334.7	560.8	18.55	0.82	0.15	767	548.3	266.0	18.67	0.78	0.34
638	267.3	277.9	18.44	0.74	0.02	703	24.0	598.1	18.55	0.91	0.90	768	135.3	789.9	18.68	0.86	0.11
639	439.9	422.5	18.44	0.81	0.15	704	272.3	288.5	18.56	0.79	0.07	769	220.5	36.5	18.69	0.83	0.05
640	395.6	148.8	18.44	0.81	0.08	705	136.4	638.7	18.56	0.82	0.12	770	190.2	450.9	18.70	0.97	0.27
641	363.8	158.0	18.44	0.77	0.08	706	319.3	809.2	18.56	0.75	−0.03	771	12.7	274.1	18.70	0.79	0.12
642	165.4	470.2	18.44	0.91	0.17	707	429.1	143.0	18.56	0.82	0.08	772	100.2	665.6	18.70	0.90	0.19
643	309.2	127.8	18.44	0.78	0.05	708	40.4	544.6	18.57	0.84	0.19	773	160.6	368.3	18.70	0.74	0.03
644	446.3	630.5	18.45	0.81	0.08	709	219.1	429.3	18.57	0.81	0.12	774	24.0	203.2	18.70	0.85	0.08
645	144.6	206.8	18.45	0.83	0.02	710	535.2	176.4	18.57	0.78	0.07	775	557.4	298.3	18.70	0.83	0.09
646	368.5	93.2	18.45	0.78	0.11	711	422.1	223.8	18.57	0.80	0.03	776	551.5	115.3	18.71	0.84	0.08
647	31.6	481.6	18.45	0.77	0.12	712	21.3	216.6	18.57	0.78	0.10	777	287.5	268.1	18.72	0.81	0.05
648	16.6	292.0	18.45	0.75	0.13	713	175.1	278.9	18.57	0.80	0.14	778	15.8	529.3	18.72	0.82	0.19
649	425.2	23.4	18.45	0.72	0.10	714	136.3	638.3	18.57	0.84	0.19	779	113.8	176.8	18.72	0.76	0.34
650	401.3	453.1	18.46	0.79	0.08	715	75.1	643.8	18.57	0.85	0.13	780	17.9	548.5	18.72	0.84	0.19

TABLE 2. (continued)

ID	X	Y	V	B − V	U − B
781	134.2	74.7	18.72	1.10	0.43
782	562.0	58.0	18.72	0.83	0.07
783	500.6	220.2	18.72	0.80	0.19
784	437.7	330.9	18.73	0.79	0.10
785	595.8	96.1	18.73	0.82	0.14
786	300.7	567.2	18.73	0.82	0.15
787	184.5	517.1	18.73	0.83	0.22
788	108.6	842.5	18.73	0.88	0.38
789	630.2	189.1	18.73	0.88	0.03
790	101.5	543.1	18.73	0.84	0.14
791	118.4	1004.6	18.74	0.87	0.06
792	346.4	37.1	18.74	0.78	0.14
793	326.3	472.8	18.74	0.83	0.19
794	454.4	587.0	18.74	0.82	0.16
795	556.1	273.3	18.74	0.83	0.10
796	285.4	461.6	18.74	0.93	0.27
797	570.7	121.1	18.74	0.83	0.09
798	425.9	34.4	18.74	0.77	0.17
799	31.1	143.7	18.74	0.71	0.11
800	335.3	499.5	18.75	0.86	0.33
801	189.8	150.7	18.75	0.92	0.23
802	189.8	855.0	18.75	0.84	0.08
803	55.0	205.6	18.76	0.86	0.19
804	511.4	298.5	18.76	0.82	0.06
805	319.4	433.2	18.76	0.85	0.15
806	247.8	835.6	18.76	0.83	0.06
807	587.5	138.5	18.77	1.05	0.76
808	310.1	86.6	18.77	0.87	0.17
809	53.2	264.6	18.77	0.81	0.16
810	345.2	537.8	18.78	0.84	0.24
811	630.9	340.9	18.78	0.81	0.24
812	145.7	407.6	18.78	1.17	1.08
813	537.0	296.1	18.78	0.83	0.17
814	317.9	532.5	18.79	0.85	0.21
815	280.8	706.6	18.79	0.81	0.13
816	527.8	351.6	18.79	0.85	0.06
817	293.7	165.2	18.79	0.67	0.25
818	353.3	123.9	18.79	0.95	0.35
819	382.3	234.2	18.80	0.82	0.11
820	364.4	349.6	18.80	0.83	0.14
821	582.3	449.9	18.80	0.87	0.15
822	68.6	129.5	18.81	0.77	0.17
823	204.1	61.7	18.81	0.79	0.14
824	225.7	178.9	18.81	0.85	0.17
825	495.5	248.5	18.81	0.85	0.10
826	36.9	16.9	18.82	0.83	0.09
827	228.1	526.2	18.82	0.83	0.17
828	351.7	447.6	18.82	0.84	0.18
829	313.9	715.6	18.82	0.82	0.11
830	291.9	113.5	18.82	0.87	0.23
831	134.6	515.2	18.82	0.87	0.46
832	140.1	679.2	18.83	0.89	0.22
833	233.7	305.1	18.83	0.81	0.17
834	168.9	113.2	18.83	0.87	0.11
835	363.7	621.3	18.83	0.84	0.17
836	18.0	475.6	18.83	0.79	0.57
837	406.0	538.0	18.83	0.95	0.20
838	44.3	453.7	18.83	0.84	0.23
839	218.2	841.9	18.84	0.77	0.20
840	401.9	570.5	18.84	0.82	0.20
841	357.0	144.5	18.84	0.82	0.14
842	60.4	503.2	18.84	0.85	0.16
843	306.6	357.2	18.85	0.92	0.29
844	445.3	147.6	18.85	1.07	0.92
845	461.8	278.4	18.85	0.59	0.24

ID	X	Y	V	B − V	U − B
846	363.2	322.5	18.85	0.82	0.17
847	537.8	42.6	18.85	0.88	0.17
848	145.5	913.2	18.85	0.84	0.14
849	175.2	29.5	18.85	1.06	0.39
850	280.4	394.5	18.86	0.82	0.14
851	217.4	264.4	18.86	0.82	0.16
852	276.1	475.0	18.87	0.68	0.37
853	320.5	359.3	18.87	0.84	0.15
854	333.9	132.2	18.87	0.85	0.14
855	535.3	3.9	18.87	0.84	0.11
856	252.4	184.8	18.88	0.84	0.19
857	150.0	261.1	18.88	0.68	0.41
858	142.3	2.7	18.88	0.79	0.11
859	615.2	256.5	18.88	0.89	0.16
860	227.2	343.8	18.88	0.87	0.13
861	200.1	513.5	18.88	0.85	0.18
862	518.3	170.8	18.89	0.81	0.15
863	333.0	772.2	18.89	0.85	0.05
864	41.8	11.8	18.90	0.83	0.11
(3) 865	408.5	331.1	18.91	1.14	0.77
866	22.7	269.9	18.91	0.84	0.10
867	313.0	510.8	18.91	0.85	0.21
868	87.1	125.3	18.91	0.79	0.18
869	583.5	505.9	18.91	0.86	0.21
870	354.0	82.1	18.91	0.85	0.14
871	231.8	409.9	18.92	0.86	0.13
872	41.0	656.8	18.92	1.69	−0.23
873	291.9	397.1	18.92	0.82	0.16
874	442.2	203.3	18.92	0.85	0.15
875	164.7	21.2	18.92	0.82	0.09
876	291.9	420.0	18.92	1.23	1.15
877	222.1	17.1	18.93	0.81	0.12
878	576.6	45.8	18.93	0.85	0.13
879	123.5	89.5	18.93	0.92	0.17
880	23.2	831.1	18.93	0.83	0.25
881	602.6	372.1	18.93	0.79	0.41
882	475.8	76.7	18.94	0.75	0.35
883	265.9	572.4	18.94	0.85	0.17
884	265.7	385.4	18.94	0.83	0.18
885	300.7	57.8	18.94	0.83	0.17
886	109.7	457.3	18.94	0.81	0.21
887	335.0	44.3	18.94	0.83	0.16
888	523.2	603.2	18.94	0.88	0.42
889	488.4	377.9	18.94	0.85	0.30
890	338.6	384.5	18.95	0.85	0.35
891	427.8	64.8	18.95	0.73	0.15
892	206.9	216.8	18.95	0.90	0.12
893	562.6	274.1	18.95	0.85	0.13
894	164.7	283.8	18.95	0.82	0.18
895	522.4	487.9	18.96	0.87	0.22
896	476.3	297.2	18.96	0.85	0.16
897	302.3	561.3	18.96	0.87	0.18
898	524.1	495.9	18.96	0.87	0.44
899	189.2	2.4	18.97	−0.34	−0.05
900	251.6	253.9	18.97	0.86	0.14
901	101.5	218.4	18.97	0.88	0.14
902	195.0	258.9	18.97	0.81	0.24
903	318.9	27.5	18.97	0.79	0.19
904	73.0	897.1	18.97	0.87	0.16
905	604.1	325.1	18.97	0.88	0.19
906	45.8	962.8	18.97	0.83	0.22
907	199.5	5.3	18.97	0.96	0.92
908	193.8	110.2	18.98	1.00	0.18
909	123.3	538.4	18.98	0.88	0.24
910	22.0	963.1	18.98	0.98	0.51

ID	X	Y	V	B − V	U − B
911	387.5	751.3	18.98	0.60	0.12
912	346.2	472.6	18.98	1.26	1.24
913	32.3	318.7	18.99	0.84	0.22
914	79.1	23.0	18.99	0.89	0.15
915	107.8	873.7	18.99	0.87	0.13
916	480.5	575.9	18.99	0.85	0.16
917	372.8	202.6	18.99	0.86	0.17
918	253.3	289.5	18.99	0.86	0.13
919	98.3	169.8	19.00	0.72	0.30
920	278.1	350.4	19.00	0.85	0.16
921	213.8	100.2	19.00	0.93	0.26
922	120.7	392.6	19.00	0.77	0.33
923	141.9	151.1	19.00	0.89	0.17
924	193.6	20.4	19.00	0.86	0.21
925	94.7	28.0	19.01	0.80	0.14
926	85.4	278.5	19.01	1.03	0.20
927	18.0	587.2	19.01	0.88	0.34
928	87.4	366.0	19.01	0.56	0.45
929	95.9	777.6	19.02	0.86	0.22
930	86.1	645.5	19.02	0.88	0.18
931	488.3	587.6	19.02	1.19	1.16
932	444.2	257.3	19.02	0.83	0.14
933	321.1	14.5	19.02	0.77	0.18
934	433.5	497.0	19.02	0.84	0.17
935	266.6	9.5	19.03	0.86	0.13
936	294.6	317.3	19.03	0.83	0.16
937	333.0	161.7	19.03	0.87	0.15
938	393.8	338.3	19.03	0.87	0.13
939	129.4	14.7	19.03	0.76	0.16
940	514.7	113.4	19.04	0.90	0.14
941	303.9	48.4	19.04	0.82	0.25
942	89.6	29.7	19.05	0.77	0.12
943	206.2	152.6	19.05	0.85	0.19
944	27.3	532.0	19.05	0.88	0.44
945	54.5	493.2	19.05	0.90	0.18
946	222.0	97.6	19.05	0.96	0.49
947	123.3	887.3	19.06	0.87	0.14
948	79.7	855.8	19.06	0.96	0.46
949	319.7	122.4	19.06	0.84	0.22
950	57.9	109.2	19.06	0.79	0.26
951	164.4	131.0	19.06	0.88	0.14
952	13.1	220.6	19.06	0.52	0.30
953	317.3	586.3	19.06	0.85	0.25
954	410.1	350.2	19.06	0.85	0.14
955	288.5	92.0	19.07	0.63	0.78
956	11.3	21.2	19.07	0.93	0.07
957	338.2	159.4	19.08	1.10	0.83
958	400.8	294.2	19.08	0.83	0.20
959	260.9	211.3	19.08	0.91	0.28
960	174.7	265.6	19.08	0.86	0.20
961	371.7	546.9	19.08	1.02	0.63
962	252.4	263.7	19.08	0.86	0.15
963	234.2	249.8	19.08	0.88	0.23
964	43.4	438.7	19.08	0.99	0.47
965	520.3	42.2	19.08	0.71	0.84
966	60.9	677.4	19.09	1.03	0.68
967	63.3	391.7	19.09	0.90	0.21
968	219.5	80.3	19.10	0.95	0.50
969	263.2	247.4	19.10	0.62	−0.02
970	52.5	366.7	19.10	0.85	0.23
971	159.7	299.5	19.10	0.85	0.32
972	126.4	413.8	19.10	0.84	0.23
973	365.8	218.4	19.11	0.90	0.19
974	482.1	44.5	19.11	0.88	0.28
975	391.7	60.9	19.11	0.87	0.14

TABLE 2. (continued)

ID	X	Y	V	B − V	U − B	ID	X	Y	V	B − V	U − B	ID	X	Y	V	B − V	U − B
976	217.2	7.1	19.11	0.92	0.45	1041	421.5	489.0	19.22	0.88	0.24	1106	435.6	345.6	19.35	0.87	0.25
977	192.9	117.7	19.11	0.97	0.17	1042	122.2	469.9	19.23	1.01	0.47	1107	214.2	447.5	19.35	0.93	0.32
978	470.5	454.4	19.11	1.41	0.34	1043	379.8	660.9	19.23	0.88	0.21	1108	440.7	246.8	19.35	0.89	0.25
979	476.9	69.5	19.11	0.95	0.43	1044	232.9	692.5	19.23	0.89	0.34	1109	166.9	931.4	19.35	0.91	0.26
980	412.2	72.0	19.11	0.86	0.28	1045	349.0	374.3	19.24	0.88	0.32	1110	79.4	320.8	19.35	0.87	0.63
981	378.1	444.5	19.11	0.87	0.29	1046	108.2	497.7	19.24	1.02	0.65	1111	514.8	240.1	19.35	0.81	0.07
982	197.8	915.0	19.11	1.12	0.80	1047	131.3	350.3	19.24	0.92	0.28	1112	531.2	52.3	19.35	0.84	0.13
983	527.5	361.6	19.11	0.85	0.17	1048	238.0	167.0	19.24	0.86	0.22	1113	561.3	499.2	19.36	0.83	0.20
984	555.9	98.9	19.12	0.90	0.35	1049	173.9	307.6	19.24	0.84	0.31	1114	379.6	494.8	19.36	0.92	0.29
985	528.7	137.5	19.12	1.03	0.45	1050	405.3	244.9	19.24	0.89	0.33	1115	159.8	168.0	19.36	0.95	0.23
986	603.2	57.2	19.12	0.86	0.32	1051	72.4	285.1	19.24	0.85	0.58	1116	349.7	103.1	19.36	0.76	0.33
987	99.9	85.9	19.12	0.69	0.45	1052	133.5	962.2	19.25	0.88	0.24	1117	288.8	238.3	19.37	0.86	0.34
988	55.7	439.5	19.12	0.89	0.34	1053	49.2	166.8	19.25	1.08	0.86	1118	618.2	20.8	19.37	0.89	0.35
989	297.6	664.5	19.13	0.85	0.22	1054	362.9	92.3	19.25	0.87	0.25	1119	373.5	536.1	19.38	0.87	0.32
990	69.7	146.1	19.13	0.85	0.14	1055	587.7	204.9	19.26	0.87	0.34	1120	401.6	263.5	19.38	0.91	0.21
991	445.5	322.0	19.13	0.82	0.17	1056	208.2	104.5	19.26	0.97	0.43	1121	154.0	205.0	19.38	0.92	0.30
992	348.6	71.6	19.13	0.95	0.57	1057	483.9	544.5	19.26	0.88	0.25	1122	400.4	549.3	19.38	0.87	0.35
993	197.6	119.0	19.14	1.22	0.35	1058	89.6	513.3	19.26	0.90	0.26	1123	237.5	345.4	19.39	0.97	0.34
994	587.6	83.9	19.14	0.85	0.18	1059	448.9	274.0	19.27	0.91	0.49	1124	332.2	233.6	19.39	0.82	0.27
995	20.5	50.0	19.14	0.87	0.17	1060	593.5	478.2	19.27	0.90	0.30	1125	231.7	387.9	19.39	1.11	0.96
996	472.1	316.3	19.14	1.03	0.70	1061	619.7	126.3	19.27	0.93	0.24	1126	186.5	400.3	19.39	0.93	0.26
997	274.0	331.6	19.14	0.85	0.55	1062	161.4	460.0	19.27	1.07	0.35	1127	301.4	330.0	19.39	0.88	0.25
998	59.2	935.0	19.14	0.92	0.22	1063	333.9	177.3	19.27	0.89	0.24	1128	270.9	369.7	19.40	1.37	1.32
999	47.7	319.1	19.14	0.87	1.04	1064	516.7	316.8	19.27	0.89	0.28	1129	20.7	382.0	19.40	0.92	0.30
1000	153.3	737.8	19.14	0.91	0.20	1065	133.9	124.7	19.27	0.92	0.23	1130	190.2	456.3	19.40	1.00	0.33
1001	346.9	265.3	19.14	0.92	0.32	1066	384.1	131.6	19.27	0.89	0.25	1131	391.6	215.9	19.41	0.91	0.27
1002	595.8	49.3	19.14	0.88	0.22	1067	380.2	243.0	19.28	0.91	0.20	1132	157.2	347.3	19.41	0.91	0.27
1003	168.3	516.8	19.14	0.86	0.58	1068	99.7	902.6	19.28	0.97	0.52	1133	456.4	89.1	19.41	1.05	0.85
1004	405.1	457.1	19.14	0.88	0.25	1069	171.5	95.2	19.28	0.93	0.24	1134	542.4	558.2	19.42	0.83	0.37
1005	630.4	296.2	19.15	0.84	0.36	1070	299.2	585.3	19.28	0.91	0.39	1135	374.0	611.8	19.42	0.80	0.23
1006	424.4	216.8	19.15	0.87	0.14	1071	610.9	308.5	19.28	0.90	0.29	1136	225.9	87.7	19.42	0.95	0.21
1007	336.6	150.7	19.15	0.89	0.18	1072	342.5	15.1	19.29	0.89	0.31	1137	449.5	319.1	19.42	0.90	0.28
1008	447.4	2.1	19.15	0.85	0.20	1073	34.3	31.2	19.29	0.87	0.27	1138	598.8	491.1	19.42	0.93	0.48
1009	104.7	64.9	19.16	0.81	0.21	1074	93.2	488.4	19.29	0.91	0.26	1139	395.0	29.1	19.42	0.84	0.42
1010	566.8	12.6	19.16	0.70	0.26	1075	42.5	184.1	19.29	0.87	0.21	1140	191.7	69.4	19.42	1.02	0.32
1011	406.2	102.7	19.16	0.88	0.16	1076	64.3	761.5	19.29	1.10	0.95	1141	36.5	539.5	19.43	1.06	0.82
1012	164.1	146.6	19.16	0.94	0.20	1077	85.6	153.8	19.29	0.78	0.37	1142	130.9	133.5	19.43	1.01	0.26
1013	278.3	364.7	19.16	0.87	0.19	1078	154.1	9.8	19.29	0.90	0.16	1143	84.6	119.6	19.43	0.86	0.26
1014	148.3	151.8	19.16	1.20	0.41	1079	467.9	184.7	19.30	1.01	0.66	1144	41.0	744.2	19.43	2.28	0.67
1015	243.4	649.3	19.16	1.56	1.33	1080	293.7	40.5	19.30	0.91	0.52	1145	360.5	311.7	19.43	0.87	0.29
1016	599.3	40.4	19.16	0.88	0.21	1081	177.7	56.2	19.30	0.78	0.52	1146	238.3	312.0	19.44	0.91	0.30
1017	60.0	212.3	19.16	0.82	0.32	1082	407.1	373.0	19.30	0.88	0.26	1147	403.8	158.3	19.44	0.93	0.25
1018	369.4	52.2	19.17	0.86	0.14	1083	445.3	500.0	19.31	0.89	0.30	1148	166.3	107.6	19.44	0.92	0.38
1019	555.0	22.9	19.17	0.80	0.12	1084	557.0	569.6	19.31	0.90	0.55	1149	488.8	121.9	19.44	0.97	0.34
1020	295.9	648.8	19.17	0.99	0.61	1085	179.4	98.6	19.31	0.92	0.27	1150	62.2	845.0	19.45	0.92	0.37
1021	242.0	208.3	19.17	0.87	0.17	1086	107.1	768.6	19.32	1.01	0.51	1151	419.4	288.8	19.45	0.90	0.25
1022	508.9	455.8	19.18	0.89	0.21	1087	94.4	981.3	19.32	1.06	0.56	(2) 1152	409.0	159.6	19.45	0.33	−0.43
1023	184.2	116.4	19.18	0.89	0.20	1088	311.9	91.1	19.32	0.89	0.22	1153	186.0	765.9	19.45	0.89	0.15
1024	228.1	267.0	19.18	0.96	0.57	1089	358.8	487.4	19.32	0.90	0.29	1154	219.6	231.3	19.46	0.89	0.36
1025	49.5	95.5	19.18	0.74	0.27	1090	625.4	70.8	19.32	1.00	0.43	1155	424.8	507.0	19.46	0.86	0.29
1026	325.2	300.9	19.18	0.96	0.50	1091	424.7	104.9	19.32	0.89	0.26	1156	86.2	149.0	19.47	0.97	0.32
1027	149.6	378.8	19.19	0.84	0.33	1092	90.2	431.5	19.32	1.07	0.48	1157	34.6	146.3	19.47	0.85	0.11
1028	16.8	639.7	19.20	0.94	0.35	1093	250.0	353.4	19.33	0.91	0.30	1158	38.3	242.4	19.47	0.84	0.80
1029	235.3	59.4	19.20	0.87	0.19	1094	544.3	201.5	19.33	0.97	0.54	1159	617.0	78.9	19.47	0.96	0.29
1030	334.9	344.0	19.20	0.86	0.16	1095	446.6	375.7	19.33	0.88	0.30	1160	624.7	400.5	19.47	0.91	0.41
1031	107.2	688.6	19.20	0.92	0.25	1096	318.6	441.7	19.33	0.89	0.35	1161	439.6	132.3	19.48	0.88	0.30
1032	582.0	172.4	19.20	0.61	0.61	1097	165.6	211.2	19.33	0.62	0.48	1162	110.3	23.2	19.48	0.90	0.26
1033	76.4	790.9	19.20	0.90	0.34	1098	295.1	377.5	19.33	0.92	0.41	1163	548.7	499.3	19.48	1.33	1.43
1034	548.6	43.5	19.21	0.94	0.25	1099	296.1	813.2	19.34	0.89	0.36	1164	482.9	319.4	19.48	0.91	0.39
1035	437.4	70.4	19.21	0.88	0.20	1100	369.3	235.2	19.34	0.85	0.21	1165	314.4	5.7	19.49	1.11	0.69
1036	441.1	193.6	19.21	0.86	0.17	1101	475.4	139.0	19.34	0.93	0.25	1166	224.9	752.7	19.49	0.93	0.31
1037	613.2	402.4	19.21	0.90	0.41	1102	175.1	434.0	19.34	1.03	0.32	1167	610.4	66.5	19.49	1.32	1.31
1038	372.2	722.5	19.21	0.89	0.18	1103	129.4	126.4	19.34	0.95	0.16	1168	349.5	233.3	19.49	0.92	0.35
1039	502.7	185.6	19.22	0.91	0.38	1104	200.8	137.9	19.34	0.93	0.19	1169	305.1	411.1	19.49	0.92	0.33
1040	276.7	541.7	19.22	0.90	0.29	1105	624.3	608.6	19.34	0.90	0.32	1170	445.9	32.2	19.49	0.90	0.34

TABLE 2. (continued)

ID	X	Y	V	B − V	U − B
1171	136.2	449.1	19.49	0.96	0.31
1172	233.2	378.6	19.49	0.93	0.38
1173	361.8	693.5	19.50	0.94	0.23
1174	218.1	356.5	19.50	0.92	0.40
1175	203.8	11.2	19.50	0.89	0.22
1176	150.4	771.5	19.50	0.93	0.33
1177	529.4	30.9	19.50	1.02	0.54
1178	342.0	570.9	19.51	0.03	−0.90
1179	87.8	624.2	19.51	0.91	0.35
1180	458.1	94.5	19.51	0.90	0.34
1181	448.9	310.7	19.51	0.91	0.28
1182	160.2	221.6	19.51	0.94	0.42
1183	398.8	616.4	19.51	0.94	0.40
1184	242.5	538.4	19.51	0.95	0.38
1185	75.1	232.5	19.51	0.88	0.58
1186	29.5	397.1	19.52	1.08	0.43
1187	595.1	77.7	19.53	0.92	0.38
1188	170.4	617.6	19.53	1.13	0.89
1189	288.9	527.5	19.53	0.93	0.47
1190	266.0	351.7	19.53	0.91	0.39
1191	317.6	699.5	19.53	1.05	0.46
1192	209.5	431.2	19.53	0.95	0.39
1193	66.7	26.6	19.55	1.14	0.53
1194	19.6	97.4	19.56	0.74	0.56
1195	277.2	294.4	19.56	0.92	0.33
1196	171.1	273.4	19.56	0.91	0.32
1197	548.1	444.0	19.57	0.81	0.12
1198	307.6	691.2	19.57	0.86	0.33
1199	92.3	334.4	19.57	1.12	1.03
1200	619.5	135.7	19.58	0.95	0.50
1201	567.2	214.6	19.58	0.96	0.31
1202	169.0	563.5	19.58	0.94	0.48
1203	463.1	140.7	19.58	0.78	0.60
1204	584.3	67.5	19.58	0.94	0.42
1205	437.9	397.5	19.59	0.83	0.45
1206	414.7	259.2	19.59	0.95	0.31
1207	216.1	225.3	19.59	0.93	0.35
1208	114.6	320.1	19.59	0.99	0.50
1209	66.3	341.0	19.59	0.91	0.41
1210	525.4	48.3	19.60	1.05	0.96
1211	481.9	60.2	19.60	0.94	0.48
1212	267.8	326.8	19.61	0.96	0.57
1213	310.4	347.4	19.61	0.92	0.38
1214	304.0	699.2	19.61	0.91	0.34
1215	460.3	499.4	19.62	0.90	0.26
1216	554.8	649.9	19.62	0.88	0.29
1217	566.6	22.9	19.62	0.80	0.10
1218	307.5	442.9	19.62	0.92	0.38
1219	388.9	656.8	19.63	0.80	0.59
1220	417.3	149.5	19.63	0.93	0.34
1221	298.9	82.8	19.63	0.88	0.57
1222	404.2	166.2	19.63	1.01	0.47
1223	522.3	393.4	19.63	0.95	0.33
1224	546.9	9.5	19.63	0.97	0.42
1225	439.0	179.2	19.64	1.13	0.90
1226	401.1	638.4	19.64	0.94	0.39
1227	167.6	625.7	19.64	0.99	0.36
1228	337.7	736.7	19.64	0.92	0.32
1229	198.4	804.7	19.64	0.94	0.37
1230	314.0	188.4	19.65	1.03	0.63
1231	127.6	639.3	19.65	0.98	0.43
1232	417.4	82.5	19.66	0.95	0.35
1233	184.1	62.5	19.66	1.12	0.39
1234	65.5	170.3	19.67	0.72	0.82
1235	315.5	165.4	19.67	0.99	0.48

ID	X	Y	V	B − V	U − B
1236	138.0	435.6	19.67	0.84	0.41
1237	249.8	116.1	19.67	0.86	0.53
1238	166.2	740.0	19.67	1.01	0.57
1239	280.2	645.7	19.67	0.94	0.36
1240	386.3	238.6	19.67	0.95	0.39
1241	20.5	913.4	19.67	0.77	0.07
1242	362.3	280.9	19.68	0.94	0.40
1243	323.4	366.5	19.68	0.78	0.03
1244	339.2	532.1	19.68	0.96	0.43
1245	449.3	75.3	19.69	0.94	0.39
1246	86.7	191.1	19.69	0.96	0.39
1247	59.2	317.3	19.69	0.94	0.51
1248	580.2	534.5	19.69	0.95	0.45
1249	611.8	228.5	19.69	0.96	0.61
1250	25.0	289.7	19.70	1.14	1.10
1251	213.9	485.6	19.70	1.06	0.37
1252	250.1	491.4	19.71	0.98	0.40
1253	202.6	566.1	19.71	0.90	0.36
1254	29.5	459.0	19.71	0.95	0.52
1255	184.8	18.4	19.72	1.13	0.47
1256	107.5	962.9	19.72	1.03	0.60
1257	453.0	118.2	19.72	1.01	0.31
1258	90.4	875.7	19.72	1.20	1.13
1259	483.3	442.4	19.72	0.97	0.51
1260	573.7	134.4	19.72	0.95	0.39
1261	612.5	428.8	19.73	0.87	0.16
1262	80.8	802.9	19.73	0.99	0.48
1263	313.3	200.2	19.73	0.95	0.44
1264	399.5	255.1	19.73	0.97	0.40
1265	102.4	27.5	19.73	0.90	0.31
1266	260.8	554.2	19.73	0.98	0.45
1267	86.6	214.5	19.74	1.04	0.59
1268	338.5	165.6	19.74	0.95	0.43
1269	117.8	317.9	19.74	0.95	0.44
1270	466.0	469.6	19.75	1.00	0.50
1271	370.4	147.0	19.75	1.12	0.92
1272	368.0	508.0	19.75	0.92	0.58
1273	619.7	476.9	19.75	1.00	0.46
1274	391.9	689.9	19.75	1.01	0.58
1275	500.0	106.3	19.75	1.04	0.49
1276	129.9	209.2	19.75	1.02	0.40
1277	370.0	532.6	19.75	1.16	1.12
1278	245.0	393.4	19.75	0.86	0.52
1279	439.5	41.8	19.75	0.32	0.30
1280	150.3	20.7	19.76	1.34	0.41
1281	526.6	430.5	19.76	1.00	0.47
1282	393.7	277.4	19.76	0.98	0.34
1283	334.5	143.0	19.77	1.00	0.39
1284	174.7	740.0	19.77	1.00	0.46
1285	622.3	365.4	19.77	0.96	0.44
1286	13.7	534.8	19.77	0.98	0.49
1287	246.5	867.7	19.77	1.22	1.29
1288	255.5	593.5	19.78	0.97	0.40
1289	391.1	623.8	19.78	1.00	0.60
1290	261.9	150.9	19.78	1.00	0.40
1291	90.2	175.2	19.78	0.84	0.51
1292	432.6	180.1	19.78	0.99	0.41
1293	498.5	96.5	19.79	0.83	0.77
1294	608.0	45.4	19.79	0.97	0.49
1295	585.2	315.5	19.79	1.07	0.84
1296	347.9	527.4	19.79	0.88	0.37
1297	437.8	229.6	19.79	0.98	0.41
1298	199.3	154.1	19.80	1.00	0.36
1299	89.3	130.6	19.80	0.94	0.37
1300	536.9	202.5	19.80	0.96	0.51

ID	X	Y	V	B − V	U − B
1301	479.7	340.6	19.81	1.10	0.43
1302	413.3	183.1	19.81	0.96	0.46
1303	355.8	589.5	19.81	0.94	0.43
1304	172.8	351.8	19.81	0.81	0.94
1305	282.0	336.3	19.81	0.98	0.40
1306	298.6	98.4	19.82	0.98	0.53
1307	629.0	31.9	19.82	1.02	0.55
1308	355.0	422.0	19.82	0.98	0.50
1309	568.9	594.5	19.83	0.95	0.49
1310	341.1	128.5	19.83	0.99	0.46
1311	30.2	273.5	19.83	1.00	0.42
1312	182.9	573.1	19.83	0.93	0.31
1313	207.5	894.2	19.83	0.94	0.35
1314	182.9	238.0	19.84	1.18	0.94
1315	451.2	500.1	19.84	0.98	0.50
1316	520.2	510.6	19.84	1.10	1.29
1317	127.2	317.9	19.84	0.90	0.40
1318	135.8	142.8	19.84	1.05	0.14
1319	177.6	83.7	19.85	1.00	0.56
1320	26.6	715.1	19.85	1.02	0.48
1321	303.2	415.5	19.85	0.95	0.49
1322	569.7	444.4	19.86	1.01	0.58
1323	125.4	651.0	19.86	0.98	0.50
1324	265.0	518.2	19.86	0.98	0.52
1325	312.6	437.3	19.86	0.99	0.42
1326	215.5	92.5	19.87	1.02	0.47
1327	136.4	120.5	19.87	1.08	0.40
1328	362.7	128.8	19.87	1.02	0.67
1329	294.0	619.0	19.87	1.00	0.49
1330	295.5	245.7	19.87	1.03	0.82
1331	599.8	261.0	19.88	1.01	0.48
1332	171.7	373.9	19.88	1.00	0.56
1333	272.2	50.1	19.88	0.92	0.58
1334	290.0	363.8	19.88	0.95	0.52
1335	437.8	221.2	19.89	1.00	0.44
1336	75.6	5.3	19.89	1.16	0.33
1337	83.5	524.8	19.90	1.01	0.45
1338	626.0	134.1	19.90	0.98	0.63
1339	110.1	300.8	19.90	0.99	0.53
1340	452.3	452.9	19.91	1.02	0.60
1341	249.9	17.3	19.91	0.94	0.60
1342	424.8	182.2	19.91	1.02	0.47
1343	524.0	559.2	19.91	1.00	0.58
1344	258.0	292.7	19.92	1.04	0.50
1345	62.1	899.6	19.92	1.00	0.55
1346	444.9	74.1	19.92	0.98	0.44
1347	191.7	385.0	19.92	0.99	0.52
1348	507.2	413.5	19.92	1.00	0.60
1349	195.9	96.7	19.92	1.08	1.03
1350	464.7	661.7	19.93	1.01	0.86
1351	486.6	280.9	19.93	1.00	0.55
1352	343.8	49.7	19.93	1.00	0.56
1353	575.0	598.2	19.93	1.18	1.20
1354	306.1	194.7	19.93	0.89	0.25
1355	186.8	776.2	19.93	1.01	0.52
1356	163.5	276.0	19.93	1.15	0.74
1357	247.1	795.4	19.93	0.98	0.51
1358	339.0	540.1	19.94	1.02	0.58
1359	69.3	270.9	19.94	1.68	1.34
1360	62.3	61.4	19.96	0.97	0.43
1361	322.6	417.6	19.96	1.15	0.80
1362	452.2	468.2	19.96	1.06	0.61
1363	120.1	827.4	19.97	1.09	0.58
1364	547.0	169.4	19.97	1.07	0.57
1365	412.6	324.7	19.98	1.38	1.42

TABLE 2. (continued)

ID	X	Y	V	B − V	U − B
1366	21.3	462.0	19.98	0.98	0.62
1367	512.0	20.2	19.98	0.98	0.56
1368	17.5	555.5	19.99	0.88	0.21
1369	454.1	643.3	19.99	0.99	0.51
1370	499.9	438.9	19.99	1.05	0.52
1371	517.8	266.8	19.99	1.01	0.52
1372	234.6	600.8	19.99	1.23	1.13
1373	496.5	194.1	19.99	0.99	0.54
1374	120.5	942.8	19.99	1.15	0.88
1375	221.8	204.3	19.99	0.99	0.66
1376	334.6	632.3	20.00	1.04	0.56
1377	117.1	208.9	20.00	0.99	0.53
1378	218.0	461.6	20.01	1.24	1.14
1379	346.6	123.1	20.01	0.82	0.09
1380	164.7	682.0	20.01	0.92	0.45
1381	98.5	118.0	20.02	0.98	0.59
1382	568.7	2.7	20.02	1.23	1.11
1383	461.3	88.4	20.02	0.93	0.64
1384	219.9	249.6	20.04	1.08	0.85
1385	532.2	147.5	20.04	0.69	0.04
1386	404.8	227.6	20.04	0.99	0.59
1387	144.1	734.4	20.04	1.38	1.28
1388	248.0	71.6	20.04	1.23	0.34
1389	525.3	57.9	20.04	1.03	0.71
1390	161.0	261.4	20.05	0.94	0.61
1391	90.4	905.2	20.05	1.04	0.60
1392	335.0	26.5	20.06	1.07	0.97
1393	137.3	110.5	20.06	1.09	0.53
1394	29.7	938.9	20.06	1.06	0.55
1395	157.2	249.6	20.06	1.29	0.47
1396	105.2	638.7	20.07	1.12	0.52
1397	405.4	614.2	20.07	1.06	0.52
1398	228.2	471.0	20.07	1.06	0.56
1399	295.7	104.1	20.08	1.05	0.66
1400	413.4	514.8	20.08	0.91	0.35
1401	86.4	404.4	20.08	1.39	0.94
1402	236.5	28.8	20.09	1.00	0.61
1403	241.1	293.0	20.10	0.98	0.16
1404	532.2	161.5	20.10	1.04	0.70
1405	28.8	249.5	20.10	0.92	0.71
1406	389.9	512.2	20.11	1.02	0.74
1407	187.4	908.0	20.11	1.02	0.54
1408	264.4	440.6	20.11	0.92	0.30
1409	111.3	522.0	20.11	0.89	0.35
1410	306.9	140.0	20.11	0.96	0.69
1411	210.0	475.1	20.11	1.01	0.49
1412	128.2	712.9	20.11	1.06	0.64
1413	142.0	585.0	20.11	0.97	0.48
1414	163.5	314.2	20.12	1.00	0.62
1415	126.4	6.3	20.12	0.98	0.76
1416	202.7	439.5	20.12	1.32	1.20
1417	240.3	555.0	20.12	1.07	0.65
1418	337.1	262.9	20.13	0.87	0.32
1419	608.3	497.1	20.13	0.96	0.46
1420	322.0	49.6	20.14	0.84	0.20
1421	215.3	533.0	20.14	1.14	0.77
1422	46.8	367.7	20.15	0.91	0.32
1423	519.1	349.6	20.15	1.10	0.60
1424	342.1	451.4	20.15	1.03	0.70
1425	108.9	733.7	20.16	1.06	0.64
1426	138.9	957.9	20.16	1.08	0.54
1427	275.1	611.5	20.16	1.21	1.16
1428	195.3	197.1	20.16	1.09	0.60
1429	532.6	368.0	20.16	0.53	1.39
1430	425.7	154.4	20.16	1.04	0.61
1431	163.1	12.7	20.17	1.69	0.76
1432	367.3	700.5	20.17	1.04	0.57
1433	539.0	455.8	20.17	0.96	0.49
1434	556.5	128.4	20.17	1.00	0.60
1435	488.3	259.4	20.18	1.53	1.41
1436	55.7	940.9	20.18	0.85	0.49
1437	608.5	606.5	20.19	1.06	0.61
1438	351.7	202.3	20.19	1.06	0.60
1439	334.7	57.7	20.19	1.09	0.58
1440	178.4	383.1	20.19	1.03	0.50
1441	245.9	215.0	20.20	1.02	0.70
1442	565.0	205.8	20.20	1.08	0.67
1443	208.7	369.8	20.20	0.99	0.73
1444	481.7	270.6	20.21	0.81	0.09
1445	613.2	121.4	20.21	1.14	0.74
1446	291.5	187.0	20.21	1.01	0.87
1447	459.5	572.8	20.21	1.05	0.71
1448	420.2	593.9	20.22	1.45	1.45
1449	469.8	29.1	20.22	1.05	0.57
1450	125.1	400.1	20.22	0.80	0.35
1451	523.6	450.5	20.23	1.21	0.95
1452	557.6	625.5	20.23	1.08	0.73
1453	377.7	460.2	20.24	1.08	0.69
1454	86.1	951.6	20.24	1.06	0.75
1455	259.3	243.8	20.25	1.07	0.62
1456	304.9	135.2	20.25	1.00	0.86
1457	424.6	292.2	20.25	1.08	0.56
1458	98.2	368.2	20.25	0.56	0.94
1459	250.3	194.8	20.25	1.14	0.66
1460	339.1	35.1	20.26	1.16	1.01
1461	423.6	260.7	20.26	1.05	0.63
1462	83.7	360.6	20.26	1.00	0.72
1463	170.1	544.3	20.27	1.01	0.91
1464	243.0	89.1	20.27	1.25	0.38
1465	95.3	608.5	20.27	1.24	1.30
1466	329.4	169.3	20.27	1.08	0.65
1467	213.8	910.6	20.27	0.75	0.82
1468	632.1	171.6	20.27	1.00	0.49
1469	251.0	404.3	20.27	1.01	0.73
1470	490.3	228.4	20.27	1.29	1.06
1471	210.3	815.2	20.27	1.15	0.79
1472	635.0	633.6	20.28	1.22	0.97
1473	50.9	59.3	20.29	1.04	0.63
1474	44.2	793.5	20.29	1.06	1.35
1475	293.8	537.0	20.29	1.05	0.71
1476	335.4	371.8	20.29	1.02	0.79
1477	512.8	414.2	20.30	0.76	0.25
1478	199.9	346.9	20.30	1.03	0.73
1479	380.2	506.5	20.30	1.00	1.05
1480	285.6	513.2	20.30	1.34	1.44
1481	341.5	653.5	20.30	1.06	0.78
1482	628.0	105.7	20.31	1.16	0.70
1483	16.7	385.4	20.32	1.16	0.84
1484	137.8	616.0	20.32	0.90	0.68
1485	229.3	868.5	20.33	0.95	0.42
1486	186.0	710.2	20.33	1.09	0.88
1487	36.8	825.2	20.33	1.01	0.62
1488	189.9	299.2	20.34	0.84	0.39
1489	305.7	581.3	20.34	1.07	0.74
1490	335.3	513.5	20.34	1.01	0.68
1491	484.6	494.9	20.34	1.09	0.78
1492	315.2	83.6	20.35	1.10	0.76
1493	309.9	306.4	20.35	1.02	0.74
1494	465.2	595.1	20.35	1.07	0.77
1495	555.0	419.6	20.36	1.07	0.77
1496	136.3	344.1	20.36	1.12	0.76
1497	28.8	579.7	20.36	1.66	1.59
1498	59.5	976.1	20.36	1.09	0.80
1499	566.6	618.9	20.36	1.02	0.63
1500	322.7	483.5	20.37	1.45	1.41
1501	430.6	159.8	20.38	1.03	0.57
1502	127.7	820.1	20.38	1.01	1.00
1503	108.3	714.8	20.38	1.04	0.69
1504	490.5	132.7	20.38	1.47	1.57
1505	498.0	472.4	20.38	1.09	0.78
1506	473.9	483.7	20.39	0.96	0.62
1507	100.0	416.0	20.39	0.64	1.09
1508	128.3	631.4	20.39	0.97	0.75
1509	305.6	174.6	20.40	1.10	0.71
1510	123.8	761.2	20.40	1.10	0.72
1511	274.1	163.4	20.41	0.47	1.40
1512	230.7	512.8	20.41	1.12	0.66
1513	63.6	200.4	20.41	1.00	0.75
1514	198.4	765.9	20.42	1.11	0.83
1515	636.3	598.6	20.42	1.11	0.87
1516	246.5	270.6	20.42	1.11	0.80
1517	520.0	194.1	20.43	1.08	0.74
1518	73.1	908.0	20.43	0.85	0.09
1519	184.2	79.1	20.43	1.48	1.15
1520	12.8	115.8	20.43	1.01	0.76
1521	549.6	161.4	20.44	1.58	1.38
1522	105.9	603.3	20.45	1.00	0.92
1523	326.8	633.8	20.45	1.12	0.72
1524	419.9	110.4	20.45	1.16	0.74
1525	384.0	302.7	20.46	0.98	0.45
1526	466.8	92.9	20.46	1.02	0.91
1527	376.8	148.3	20.46	1.06	0.70
1528	169.3	143.0	20.46	1.31	0.73
1529	437.4	408.2	20.46	0.96	0.34
1530	205.1	249.1	20.47	1.15	0.83
1531	472.7	208.0	20.47	1.24	0.81
1532	621.4	376.7	20.48	1.09	0.75
1533	185.4	138.9	20.48	1.28	0.68
1534	55.0	815.2	20.48	1.12	0.86
1535	341.4	221.5	20.49	1.04	0.81
1536	266.5	614.2	20.49	1.09	0.89
1537	498.8	68.4	20.50	0.73	1.42
1538	289.9	368.9	20.50	1.07	0.71
1539	43.8	568.8	20.51	1.01	0.67
1540	162.3	962.0	20.51	1.16	0.83
1541	263.8	146.5	20.51	1.24	0.65
1542	329.8	42.2	20.51	1.09	0.66
1543	255.2	132.0	20.51	1.28	0.64
1544	69.8	362.6	20.52	1.09	0.91
1545	48.0	294.9	20.53	1.16	0.85
1546	304.9	513.3	20.53	1.12	0.87
1547	63.3	119.9	20.53	1.01	0.88
1548	535.4	331.4	20.54	0.98	1.00
1549	509.5	232.2	20.54	1.12	0.79
1550	330.1	643.8	20.54	1.09	0.87
1551	425.6	125.0	20.54	0.96	0.37
1552	382.5	219.4	20.55	1.09	0.95
1553	305.8	102.9	20.55	1.08	0.87
1554	595.6	403.4	20.55	1.15	1.10
1555	19.5	415.6	20.55	1.25	1.25
1556	585.6	250.6	20.55	1.11	0.82
1557	165.0	509.7	20.55	0.90	1.64
1558	170.9	857.7	20.56	1.07	0.75
1559	526.2	40.6	20.56	0.99	1.13
1560	570.4	572.7	20.57	0.03	−0.90

TABLE 2. (continued)

ID	X	Y	V	B − V	U − B	ID	X	Y	V	B − V	U − B	ID	X	Y	V	B − V	U − B
1561	56.0	839.4	20.58	1.10	0.85	1626	397.8	385.4	20.78	1.06	1.14	1691	435.9	627.0	21.07	1.14	1.47
1562	599.2	452.6	20.58	1.12	0.90	1627	25.3	498.5	20.78	0.96	1.26	1692	337.0	358.6	21.07	1.13	1.52
1563	70.2	776.9	20.58	0.99	0.39	1628	395.8	459.3	20.79	1.76	0.93	1693	39.2	379.0	21.08	1.28	1.09
1564	53.4	55.3	20.58	1.04	0.73	1629	444.8	175.5	20.79	1.23	0.86	1694	629.3	603.6	21.09	1.16	1.02
1565	222.5	352.6	20.59	1.59	1.52	1630	212.0	157.8	20.79	1.20	0.87	1695	313.8	230.2	21.10	1.19	1.09
1566	322.5	376.9	20.59	1.04	0.99	1631	156.9	382.4	20.80	1.06	1.70	1696	237.6	140.0	21.11	1.40	0.89
1567	576.0	178.3	20.59	0.80	1.29	1632	12.9	610.9	20.81	1.22	1.11	1697	524.7	647.5	21.11	0.45	2.19
1568	350.3	765.6	20.59	1.11	0.86	1633	277.8	203.4	20.83	1.03	1.22	1698	461.0	434.1	21.11	1.03	0.85
1569	327.4	568.5	20.60	1.08	0.85	1634	436.2	184.6	20.83	1.38	1.03	1699	324.6	403.0	21.12	1.23	1.18
1570	264.7	718.9	20.60	1.08	0.83	1635	84.0	312.7	20.84	1.11	0.73	1700	53.5	677.3	21.12	1.27	1.17
1571	286.9	182.5	20.60	1.04	1.08	1636	445.7	589.5	20.85	1.21	0.91	1701	21.4	173.0	21.12	1.23	0.89
1572	533.4	429.3	20.60	1.14	0.88	1637	259.9	619.1	20.85	1.29	1.74	1702	377.5	209.9	21.14	1.25	1.58
1573	199.7	91.2	20.60	0.95	0.12	1638	228.0	396.1	20.85	1.37	1.33	1703	285.0	719.2	21.14	1.20	1.23
1574	263.1	424.1	20.61	1.17	0.82	1639	596.6	285.9	20.85	1.20	0.97	1704	541.1	399.3	21.15	1.14	1.31
1575	361.4	137.2	20.61	1.12	0.87	1640	331.8	301.6	20.86	1.12	1.07	1705	320.7	82.9	21.16	1.22	1.17
1576	123.8	972.6	20.61	1.19	0.96	1641	291.1	789.2	20.86	1.13	0.92	1706	231.4	200.5	21.18	1.35	1.37
1577	162.2	913.7	20.62	1.16	0.96	1642	90.9	238.8	20.87	1.48	0.90	1707	612.8	540.5	21.19	1.25	1.23
1578	470.8	229.8	20.62	1.12	0.89	1643	510.4	132.3	20.88	1.54	1.30	1708	238.5	417.6	21.19	1.58	1.49
1579	364.2	435.4	20.62	1.17	0.79	1644	480.0	407.7	20.88	1.03	1.39	1709	504.1	341.9	21.20	1.63	1.17
1580	62.6	693.1	20.62	1.09	0.85	1645	100.6	869.6	20.88	1.10	0.83	1710	390.1	32.6	21.23	1.07	1.16
1581	339.4	179.0	20.63	1.19	0.85	1646	566.0	647.7	20.89	1.06	0.98	1711	434.2	576.9	21.23	1.09	0.99
1582	592.1	129.9	20.63	1.15	0.90	1647	305.4	475.1	20.89	1.14	1.46	1712	348.6	305.2	21.24	1.20	1.01
1583	422.9	253.2	20.63	1.11	0.95	1648	429.8	259.6	20.89	1.32	1.51	1713	229.5	162.9	21.26	1.41	1.13
1584	228.7	59.5	20.63	1.10	0.91	1649	182.5	617.8	20.90	1.54	1.13	1714	445.3	445.0	21.26	1.54	1.20
1585	577.3	272.2	20.63	1.16	0.90	1650	243.5	55.9	20.90	1.25	1.01	1715	99.7	338.8	21.26	1.10	1.03
1586	100.8	142.5	20.64	0.26	0.57	1651	151.2	171.8	20.90	1.30	1.05	1716	282.7	329.3	21.26	1.30	0.88
1587	45.1	162.9	20.64	1.09	0.91	1652	233.3	65.6	20.90	1.11	0.82	1717	558.2	66.5	21.26	1.37	0.99
1588	170.2	538.8	20.64	1.25	1.98	1653	244.5	353.7	20.91	1.29	0.99	1718	549.6	234.4	21.27	0.88	0.17
1589	125.7	901.3	20.64	1.09	1.16	1654	74.2	86.8	20.92	1.07	1.51	1719	75.0	709.4	21.27	1.12	1.09
1590	146.6	850.5	20.65	1.10	0.90	1655	530.8	474.4	20.92	1.22	1.04	1720	315.8	664.3	21.27	1.22	1.00
1591	339.1	647.8	20.66	1.18	0.96	1656	350.1	363.4	20.93	1.24	1.16	1721	213.5	687.6	21.27	1.13	1.20
1592	554.8	401.4	20.66	1.21	0.81	1657	208.4	334.6	20.94	1.32	0.87	1722	537.9	597.5	21.27	0.83	0.13
1593	631.7	532.2	20.66	1.18	0.96	1658	246.7	134.3	20.94	1.43	0.69	1723	87.7	751.9	21.28	1.15	0.83
1594	213.4	247.7	20.67	1.16	0.89	1659	449.8	171.8	20.95	1.31	1.22	1724	243.3	473.9	21.29	1.24	1.17
1595	257.6	394.1	20.67	0.92	0.26	1660	401.8	607.8	20.95	1.24	1.10	1725	391.4	459.9	21.29	1.30	1.30
1596	559.4	378.7	20.68	0.86	1.40	1661	324.4	389.9	20.95	1.09	1.24	1726	32.9	173.4	21.30	1.36	1.21
1597	432.9	929.4	20.68	1.11	2.45	1662	350.6	208.5	20.95	0.67	1.53	1727	581.3	423.7	21.30	0.52	0.00
1598	431.6	219.6	20.68	1.23	0.90	1663	400.9	416.1	20.96	0.97	1.13	1728	551.3	85.9	21.30	1.62	1.62
1599	385.7	156.8	20.69	0.97	0.80	1664	20.1	80.8	20.96	0.80	1.38	1729	288.3	771.8	21.31	1.34	1.35
1600	26.7	412.1	20.69	0.99	1.05	1665	323.0	351.2	20.96	1.19	1.20	1730	65.8	111.4	21.31	1.07	1.24
1601	232.8	224.4	20.69	1.10	0.77	1666	259.9	492.5	20.97	1.30	1.27	1731	491.0	242.2	21.32	1.44	1.21
1602	546.7	520.6	20.69	1.14	1.23	1667	298.4	112.6	20.97	1.13	1.14	1732	362.1	410.3	21.32	1.00	0.36
1603	559.2	180.9	20.70	1.01	0.85	1668	336.3	215.3	20.97	1.01	0.66	1733	619.6	636.0	21.33	1.07	0.62
1604	631.0	407.3	20.70	0.86	0.04	1669	112.7	702.8	20.98	1.05	0.44	1734	224.5	666.5	21.33	0.77	2.51
1605	521.8	102.7	20.71	0.90	1.10	1670	267.6	776.6	20.98	0.83	0.01	1735	103.4	492.8	21.33	1.36	1.21
1606	217.5	302.3	20.71	1.38	1.66	1671	446.2	429.7	20.99	1.10	0.75	1736	260.1	36.7	21.35	1.30	1.02
1607	544.6	600.2	20.71	1.28	1.48	1672	65.0	737.3	20.99	1.25	1.12	1737	514.0	255.8	21.35	1.35	1.15
1608	415.5	557.9	20.71	1.20	1.07	1673	438.8	323.3	20.99	1.23	1.13	1738	33.0	693.3	21.35	1.20	0.99
1609	244.1	324.9	20.73	1.10	1.03	1674	52.8	483.3	20.99	2.04	1.22	1739	199.8	163.3	21.36	1.67	1.09
1610	160.1	650.8	20.73	1.18	1.10	1675	471.5	548.2	20.99	1.22	1.10	1740	88.2	505.5	21.37	1.40	0.91
1611	400.4	205.1	20.73	1.13	1.07	1676	337.9	487.9	21.00	1.25	1.19	1741	60.9	123.8	21.37	1.15	1.19
1612	389.3	100.1	20.73	1.15	1.09	1677	60.6	416.8	21.00	1.15	1.60	1742	544.3	616.2	21.38	1.27	1.70
1613	277.5	256.3	20.74	1.13	0.96	1678	237.6	489.4	21.00	1.23	1.33	1743	64.7	349.2	21.40	1.29	1.40
1614	233.8	320.0	20.74	1.26	1.06	1679	115.7	128.5	21.00	1.23	0.82	1744	226.4	563.4	21.41	1.35	1.38
1615	450.5	382.5	20.74	0.95	1.43	1680	397.9	198.9	21.01	0.70	0.75	1745	334.9	674.4	21.42	1.01	0.22
1616	572.9	383.4	20.74	1.21	1.18	1681	212.4	164.4	21.01	1.15	0.39	1746	514.0	177.3	21.43	0.52	0.82
1617	53.0	328.1	20.74	1.14	1.05	1682	364.6	384.2	21.01	1.22	1.28	1747	130.1	737.7	21.43	1.10	0.47
1618	594.0	88.2	20.75	1.47	1.27	1683	564.1	566.2	21.03	1.14	1.35	1748	383.9	163.6	21.43	1.37	1.31
1619	539.2	253.2	20.75	1.27	0.92	1684	573.9	587.8	21.03	1.23	0.96	1749	124.9	858.2	21.43	1.37	1.16
1620	492.3	358.4	20.75	1.54	1.45	1685	327.9	263.4	21.04	1.23	0.84	1750	326.9	557.1	21.44	1.38	1.35
1621	87.5	766.0	20.76	1.46	1.35	1686	608.3	529.4	21.05	1.15	1.10	1751	94.1	686.5	21.44	1.43	1.26
1622	607.2	72.3	20.77	1.22	0.89	1687	20.8	34.6	21.05	1.45	1.13	1752	620.3	330.3	21.44	1.48	1.44
1623	27.4	285.5	20.77	1.07	1.20	1688	18.3	649.2	21.06	1.50	1.51	1753	519.0	63.7	21.45	1.37	1.74
1624	386.4	781.8	20.77	1.10	1.07	1689	15.2	167.8	21.06	1.17	0.83	1754	208.8	244.6	21.49	1.25	1.37
1625	71.8	300.3	20.78	1.15	1.03	1690	333.8	691.2	21.07	0.96	0.28	1755	453.6	748.2	21.49	1.60	1.84

TABLE 2. (continued)

ID	X	Y	V	B − V	U − B
1756	224.6	261.0	21.49	1.42	1.14
1757	217.8	873.1	21.50	1.42	1.22
1758	75.1	702.5	21.51	1.36	1.28
1759	388.8	352.2	21.51	1.41	1.46
1760	481.7	561.9	21.51	0.83	0.28
1761	27.1	587.0	21.52	1.42	1.14
1762	383.7	550.5	21.52	0.98	0.33
1763	110.8	757.4	21.52	1.40	1.38
1764	508.5	616.5	21.53	1.88	1.42
1765	464.9	360.5	21.53	1.11	0.81
1766	244.6	286.0	21.54	1.40	1.41
1767	592.0	965.0	21.55	1.72	1.70
1768	416.9	446.9	21.55	1.78	1.51
1769	214.2	539.9	21.56	1.48	1.37
1770	214.3	649.1	21.56	2.40	1.18
1771	307.3	928.2	21.57	1.37	1.20
1772	389.1	271.3	21.59	1.49	1.01
1773	131.0	898.3	21.59	1.34	1.22
1774	293.2	515.7	21.60	1.39	1.30
1775	236.6	508.5	21.61	1.11	0.73
1776	57.5	856.2	21.62	1.48	1.33
1777	426.8	228.2	21.62	1.00	0.34
1778	595.0	419.7	21.62	1.14	2.21
1779	353.5	313.7	21.62	1.13	0.70
1780	93.0	697.4	21.63	1.21	0.93
1781	82.2	960.3	21.63	1.01	0.20
1782	203.9	391.2	21.66	1.15	0.78
1783	361.2	579.6	21.66	1.33	1.05
1784	601.7	142.2	21.67	1.24	1.29
1785	269.2	296.3	21.67	1.64	1.16
1786	457.4	874.0	21.67	1.13	1.17
1787	238.6	152.8	21.67	1.43	1.41
1788	339.1	443.7	21.68	1.24	1.60
1789	454.7	167.2	21.69	1.41	1.97
1790	527.0	182.4	21.70	1.27	1.41
1791	312.9	835.3	21.70	1.09	0.83
1792	178.3	940.9	21.71	1.42	1.56
1793	181.9	751.8	21.71	1.18	1.68
1794	222.2	254.8	21.72	1.43	1.78
1795	27.2	300.7	21.72	1.09	−0.10
1796	89.2	327.5	21.74	1.42	1.30
1797	614.1	41.4	21.75	1.49	2.04
1798	444.0	278.8	21.76	1.04	0.47
1799	411.5	469.2	21.78	1.10	0.62
1800	169.6	254.2	21.79	1.15	1.14
1801	213.3	519.2	21.82	1.14	1.22
1802	531.6	615.6	21.83	2.98	0.47
1803	254.3	719.0	21.87	1.79	1.42
1804	359.1	615.6	21.87	1.55	1.29
1805	566.0	304.0	21.88	1.35	1.03
1806	206.9	557.1	21.90	1.56	1.54
1807	338.4	746.0	21.90	1.41	1.82
1808	352.3	613.2	21.92	0.88	−0.04
1809	528.4	907.5	21.92	1.40	1.53
1810	185.7	725.2	21.93	1.39	0.92
1811	202.9	578.8	21.94	1.21	1.58
1812	66.4	787.0	21.95	0.84	0.24
1813	421.1	235.3	21.95	1.58	1.68
1814	617.9	235.4	21.96	0.36	0.44
1815	232.9	270.5	21.97	0.88	0.19
1816	547.8	790.1	21.97	1.35	1.21
1817	269.9	309.6	21.99	1.77	0.99
1818	363.5	965.3	22.01	1.37	1.68
1819	40.1	193.3	22.06	0.79	0.43
1820	339.1	115.7	22.07	1.34	1.50
1821	197.4	353.5	22.09	1.16	1.35
1822	87.5	894.4	22.09	1.31	1.38
1823	94.2	866.0	22.11	1.40	1.35
1824	100.2	572.5	22.11	0.85	1.07
1825	589.4	37.3	22.11	1.54	1.51
1826	139.6	942.1	22.12	1.34	1.06
1827	354.7	994.6	22.14	1.81	1.08
1828	315.1	310.5	22.15	1.64	1.51
1829	405.4	272.2	22.20	1.35	0.49
1830	260.0	941.9	22.20	1.51	0.97
1831	18.8	678.2	22.21	1.07	0.83
1832	51.9	648.9	22.22	1.47	1.12
1833	611.3	522.8	22.24	1.36	0.71
1834	611.7	637.2	22.25	1.70	1.24
1835	616.6	300.9	22.26	1.21	0.48
1836	353.7	226.5	22.28	1.04	1.64
1837	162.5	564.3	22.29	1.24	1.61
1838	234.5	714.7	22.30	0.94	1.16
1839	390.9	720.6	22.31	1.71	0.51
1840	587.3	44.4	22.32	1.26	1.35
1841	27.5	692.4	22.32	1.53	1.35
1842	393.2	742.1	22.32	2.32	0.22
1843	286.3	379.5	22.38	1.71	1.16
1844	383.6	212.1	22.39	1.39	1.36
1845	573.5	396.2	22.50	1.22	1.14
1846	29.3	847.1	22.53	1.61	0.98
1847	241.2	231.2	22.55	1.72	1.04
1848	255.3	663.8	22.57	1.36	0.85
1849	466.1	328.7	22.63	2.00	0.86
1850	288.6	447.1	22.64	0.43	−0.89
1851	270.3	893.1	22.66	1.44	0.86
1852	510.8	785.5	22.97	1.45	1.04
1853	102.8	984.7	22.99	1.57	0.73
1854	122.3	800.3	23.00	1.14	0.88
1855	553.7	37.2	23.07	2.76	−0.42
1856	339.1	978.5	23.29	1.79	0.19
1857	133.4	909.6	23.33	0.55	−0.06
1858	633.7	861.2	23.65	0.31	−0.63
1859	631.5	923.6	24.05	1.07	−0.31
1860	325.8	753.4	24.56	−0.41	−0.21
1861	379.7	342.9	24.84	−0.18	−0.71

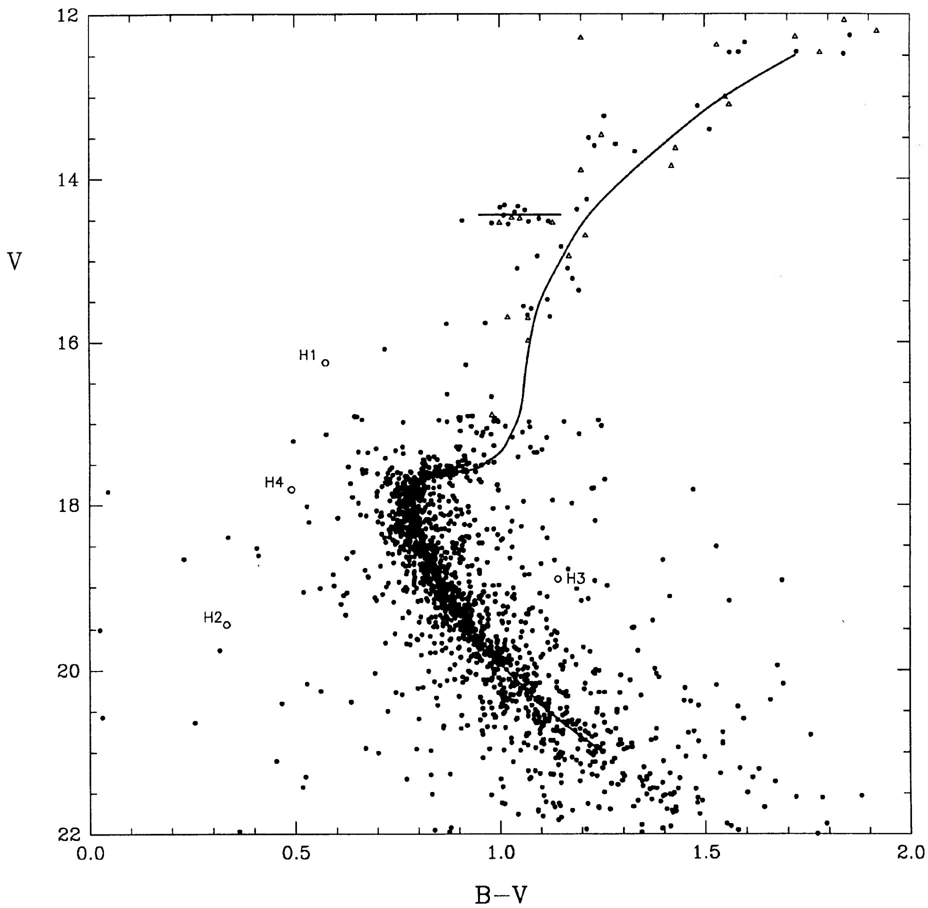

FIG. 1. The color–magnitude diagram obtained for M71. The photometry is listed in Table 2. Stars listed in Arp and Hartwick's Table 1 in the vicinity of the giant branch are shown as open triangles. Variables are shown as open circles and are labeled (see text). The fiducial derived from this diagram is shown as the solid line. Reddening corrections have not been applied to the data in this diagram.

& Hartwick's (1971) Fig. 3 and Table 2(a) we find a similar result of $V_{HB} = 14.44 \pm 0.08$. For comparison purposes the stars measured photoelectrically by Arp and Hartwick and listed in their Table 1 that lie in the red giant branch region are plotted as open triangles in Fig. 1. The variable star candidates discussed in Sec. 4 are plotted as open circles. The solid curve is the adopted fiducial, which was drawn by hand through the highest density of points and is in reasonable agreement with Arp and Hartwick's fiducial—though it should be pointed out that their photoelectric study is not necessarily complete. Unfortunately, Cudworth's magnitude limit is approximately 1 mag brighter than the turn-up point of the subgiant branch and the location of this point is critical for most age determination methods, as will be seen in Sec. *3.2* (see also VandenBerg *et al.* 1990).

Figure 2 is a finding chart for the stars in Table 2 and was produced using that data. The completeness of this map is thus dependent on the ability of DAOPHOT to find faint stars and accurately measure their magnitudes. Comparison of Fig. 2 with Richer & Fahlman's (1988) Fig. 1 shows a very good agreement.

Our estimate of the M71 fiducial is tabulated in Table 3, columns (1) and (2). Table 2 does not include errors in the magnitudes and colors of the stars—we include in columns (3) and (4) of Table 3 typical error values in each magnitude bin, and the corresponding error in $B-V$ color at that point. These values are the median errors in V and $B-V$ for the stars contained in the bin whose center lies at the appropriate entry in the table.

3.2 Comparison with 47 Tucana

VandenBerg *et al.* (1990) have recently demonstrated the effectiveness of a new method of relative age determinations. Their procedure involves shifting fiducials of two clusters so that the colors of the turn off points, and the magnitudes at points on the main sequence $0^m.05$ redder than the turnoff colors, are matched together. If the two clusters are of similar metallicity then any difference in the color of the giant branches can be interpreted as an age difference. Sarajedini & Demarque (1990) have proposed a similar scheme in which the difference in color between the turnoff and the base of the subgiant region is used to estimate ages, allowing age differences to be computed fairly easily.

47 Tuc is a globular cluster similar in many respects to M71. Hesser *et al.* (1987, hereafter referred to as H87) adopt a metallicity for 47 Tuc of -0.65, and discuss the reasoning behind this choice. Metallicity (defined here to mean [Fe/H]) estimates for M71 range from -0.4 (Bessell 1983) to -1.2 (Cohen 1980, using echelle spectra). Leep *et al.* (1987) restrict the value to between -0.6 and -1.0. As shall be seen below, theoretical isochrones computed for an $[Fe/H] = -0.78$ provide a good fit to our M71 fiducial,

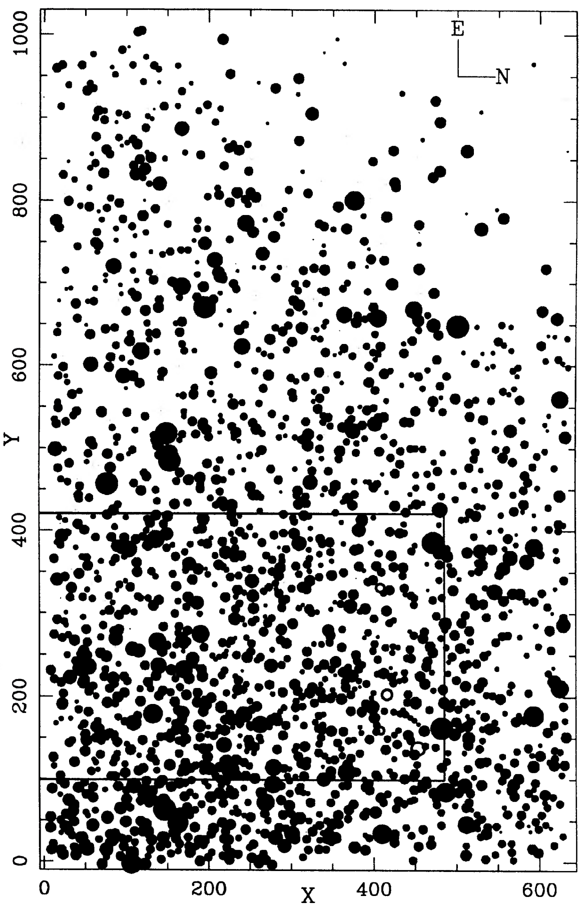

FIG. 2. Identification chart for the large field photometry. This map was constructed using the photometry list given in Table 2, and is therefore not guaranteed to be complete. The field used to search for variables is the area enclosed by the solid lines in the southwest portion of the figure. The variables themselves (discussed in Sec. 4 of the text) are marked as open circles. The plate scale is 0".21 per pixel.

TABLE 3. M71 fiducial sequence.

V	$B-V$	ϵ_V	ϵ_{B-V}
12.50	1.72	0.04	0.06
13.00	1.55	0.04	0.07
13.50	1.42	0.04	0.06
14.00	1.305	0.04	0.06
14.50	1.21	0.04	0.06
15.00	1.15	0.04	0.06
15.50	1.10	0.04	0.06
16.00	1.075	0.04	0.06
16.50	1.06	0.04	0.06
17.00	1.04	0.04	0.06
17.20	1.02	0.04	0.06
17.40	0.99	0.04	0.06
17.50	0.96	—	—
17.57	0.93	—	—
17.58	0.92	—	—
17.60	0.875	0.01	0.01
17.63	0.835	—	—
17.73	0.795	0.03	0.04
17.80	0.785	0.01	0.01
17.90	0.777	0.01	0.01
18.00	0.775	0.01	0.02
18.20	0.78	0.01	0.01
18.40	0.793	0.01	0.01
18.60	0.815	0.01	0.01
18.80	0.836	0.01	0.01
19.00	0.86	0.01	0.01
19.20	0.885	0.01	0.02
19.40	0.915	0.01	0.01
19.60	0.945	0.01	0.02
19.80	0.98	0.01	0.01
20.00	1.015	0.01	0.02
20.20	1.055	0.01	0.02
20.40	1.095	0.01	0.02
21.00	1.25	0.02	0.03

though the [Fe/H] = − 0.65 isochrones also fit relatively well.

Following the VandenBerg *et al.* technique [and noting the caveats for this procedure mentioned there and in VandenBerg & Stetson (1991)] we have performed a comparison between 47 Tuc and M71 which is shown in Fig. 3. The 47 Tuc fiducial is the published fiducial of H87, shifted by + 0.379 in V and + 0.235 in $B-V$. These shifts are very close to the difference in distance moduli $[(M-m)_{\rm M71}-(M-m)_{\rm 47\ Tuc}=0.4]$ and reddening $[{\rm E}(B-V)_{\rm M71}-{\rm E}(B-V)_{\rm 47\ Tuc}=0.24]$ for the two clusters, using the results published by Richer & Fahlman (1988) and H87. The agreement between the two fiducials is readily apparent. The small difference between the giant branches from $14<V<16$ may be due merely to our estimate of the poorly defined M71 fiducial; indeed, the 47 Tuc fiducial does not seem out of place when plotted on the M71 color–magnitude diagram. Arp & Hartwick (1971) sketched a very similar fiducial—in their Fig. 3 the turnoff color is at $B-V=0.76$ and the base of the giant branch is at $B-V=1.00$. This agrees very well with the fiducial presented here. We do not, therefore, find any convincing evidence for a substantial age difference between M71 and 47 Tuc. This conclusion is contrary to the result reported by Heasley & Christian (1991), that M71 is ~3 Gyr older than 47 Tuc. However, it must be stressed that our conclusion depends critically on the fiducial location at and just above the base of the red giant branch. It is clear from Fig. 1 that our fiducial is not well defined in that region. Consequently we cannot firmly exclude the possibility of a relative age difference between 47 Tuc and M71.

Figure 4 compares M71 with oxygen enhanced theoretical isochrones computed by Bergbusch & VandenBerg (1991). In both (a) and (b) the isochrones have been shifted using a distance modulus of 13.7 and a reddening of 0.28. An additional shift in $B-V$ of 0.015 was required to match the fiducial with the isochrones. Figure 4(a) compares the fiducial to the isochrones. Below the turnoff the agreement between observation and theory is good, but at the turnoff the fiducial crosses between the 14 and 16 Gyr isochrones. This mismatch, together with that evident along the giant branch is, at least in part, due to the difficulty of defining the fiducials with sparse and scattered data. In Fig. 4(b) we plot the isochrones over the individual points in the color–magnitude diagram defined by our photometry. It can be seen that

TABLE 4. Photometry for H1, H2, H3, and H4.

HJD[a] (2446200.0+) (1)	Filter (2)	H1 (3)	H2 (4)	H3 (5)	H4 (6)	HJD[a] (2446200.0+) (1)	Filter (2)	H1 (3)	H2 (4)	H3 (5)	H4 (6)
58.86377	V	16.237	19.522	18.866	17.607	59.89504	B	16.828	19.853	20.032	18.348
58.86768	V	16.247	19.474	18.878	17.617	59.90285	B	16.821	19.801	20.054	18.333
58.87158	V	16.257	19.458	18.886	17.620	59.91067	B	16.804	19.757	20.021	18.342
58.87549	V	16.269	19.437	18.904	17.631	59.91848	B	16.807	19.746	20.002	18.355
58.87939	V	16.287	19.414	18.925	17.637	59.92629	B	16.839	19.787	19.993	18.381
58.88330	V	16.289	19.394	18.943	17.659	59.93410	B	17.137	19.853	19.964	18.394
58.88721	V	16.293	19.446	18.966	17.664	59.94582	B	16.844	19.835	19.946	18.404
58.89502	V	16.284	19.379	18.998	17.673	60.08645	V	16.309	—	—	17.843
58.89893	V	16.273	19.396	19.028	17.672	60.09036	V	16.303	—	18.782	17.782
58.90283	V	16.221	19.447	19.049	17.670	61.04350	B	16.811	19.846	19.979	18.324
58.90674	V	16.205	19.468	19.051	17.669	61.05132	B	16.770	19.780	19.927	18.313
58.91064	V	16.198	19.502	19.045	17.676	61.05913	B	16.786	19.778	19.950	18.318
58.91455	V	16.218	19.487	19.029	17.665	61.06694	B	16.804	19.771	19.923	18.309
58.91846	V	16.238	19.523	18.999	17.666	61.93024	V	16.282	19.465	18.914	17.795
58.92236	V	16.261	19.493	18.967	17.648	61.93805	V	16.299	19.499	18.891	17.921
58.92627	V	16.299	19.481	18.928	17.634	61.94196	V	16.303	19.514	18.881	18.012
58.93408	V	16.233	19.397	18.864	17.592	61.94587	V	16.299	19.521	18.888	18.113
58.95361	V	16.209	19.403	18.869	17.582	61.95368	V	16.269	19.488	18.874	18.233
58.95752	V	16.187	19.447	18.868	17.575	61.95758	V	16.222	19.465	18.859	18.270
58.96143	V	16.200	19.433	18.865	17.581	61.96149	V	16.197	19.417	18.853	18.292
58.96533	V	16.200	19.499	18.851	17.583	61.96540	V	16.183	19.407	18.837	18.289
58.97314	V	16.234	19.488	18.864	17.582	61.96930	V	16.173	19.367	18.860	18.237
58.97705	V	16.248	19.491	18.842	17.576	61.97321	V	16.218	19.392	18.826	18.267
59.03174	B	16.830	19.831	19.946	18.281	61.97712	V	16.248	19.382	18.825	18.201
59.04346	B	16.822	19.878	19.937	18.309	61.98103	V	16.286	19.406	18.830	18.076
59.05127	B	16.869	19.636	19.975	18.311	61.98884	V	16.303	19.414	18.823	17.986
59.05909	B	16.819	19.791	20.022	18.279	61.99274	V	16.317	19.451	18.840	17.914
59.06690	B	16.882	19.757	19.985	18.389	61.99665	V	16.308	19.464	18.818	17.842
59.08643	B	16.845	19.784	20.218	18.308	62.02399	B	16.710	19.697	20.076	18.082
59.09424	B	16.815	19.800	20.267	18.297	62.03181	B	16.815	19.736	19.996	18.308
59.10205	B	16.784	19.954	20.241	18.323	62.03962	B	16.850	19.713	20.002	18.304
59.10987	B	16.815	19.944	20.061	18.350	62.04743	B	16.858	19.747	20.015	18.304
59.85598	B	17.311	19.740	20.228	18.364	62.05524	B	16.843	19.728	20.057	18.304
59.86379	B	16.820	19.764	20.146	18.377	62.06306	B	16.817	19.821	20.128	18.296
59.87942	B	16.798	19.847	20.067	18.362	62.07087	B	16.800	19.838	20.246	18.458
59.88723	B	16.811	19.869	20.035	18.350	62.07868	B	16.818	19.796	20.276	18.284
						62.08649	B	16.839	19.755	20.192	18.302

a) Heliocentric Julian Date of mid exposure

the isochrones do fit the data reasonably well and the absolute age of M71 appears to be between 14 and 16 Gyr. H87 derive an absolute age of 13.5 ± 2 Gyr for 47 Tuc using isochrones with $[Fe/H] = -0.65$. To within the limits of our data we find a similar age for M71. This conclusion, which depends upon the adopted values of the reddening and distance modulus, is clearly consistent with the result of comparing the fiducials of 47 Tuc and M71. (Note that the fiducial comparison is independent of distance and reddening uncertainties and requires only that the clusters have a similar chemical composition.)

4. VARIABLE STARS IN M71

4.1 Variable Star Identification

The major purpose of this work was to search for variable stars. Although automated schemes for selecting variables from a set of data have been proposed (e.g., Shara *et al.* 1988) we found it necessary to view the light curve of each star in order to pick out the variables. This leads to the possibility of having not correctly identified some small amplitude variables.

A total of four variables were discovered in the field under investigation. Photometry for these stars is given in Table 4. Each of these will be discussed in turn, following a brief description of the method used to analyze the periods.

Two of the variables discovered had sufficient phase coverage to allow the use of a Fourier analysis technique to determine their periods. The approach used followed that of Deeming (1975), as modified by Kurtz (1985), and Mathews & Wehlau (1985). This latter modification uses trigonometric identities to reduce computing time when calculating the Fourier components. The program used for this analysis was supplied by J. M. Matthews, and subtracts the mean of the dataset so as to remove any long term trends (as noted in Deeming's paper) before the analysis commences. The usual approach adopted for this work was to first conduct an initial period analysis over a fairly wide range of frequencies; here 0–100 cycles per day (c/d) with a grid of 2000 frequencies. Then a more detailed analysis using a finer frequency grid was used to narrow down onto the most prominent peaks. Although there was often sufficient phase coverage to determine a period in this way, the lack of an extended temporal baseline of observations led to aliasing

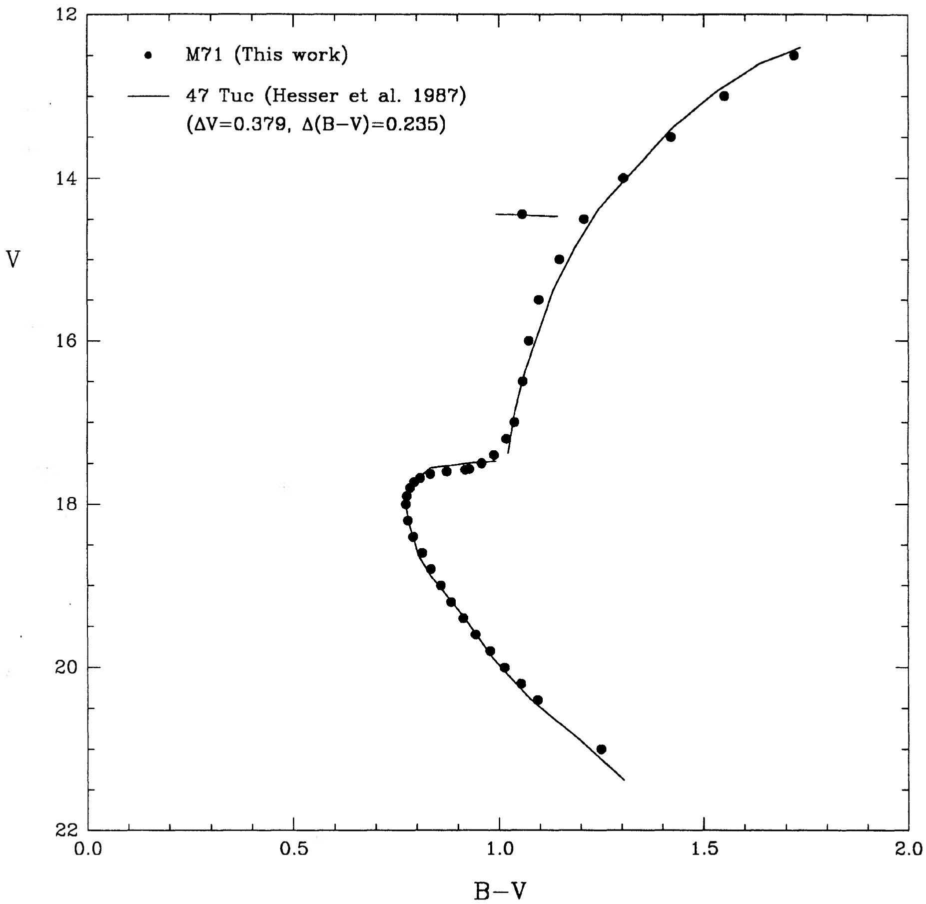

FIG. 3. A comparison between the principle sequences of M71 (solid curve, from the current work) and 47 Tuc (dashed curve, from Hesser *et al.* 1987). The latter have been shifted by 0.379 in V and 0.235 in $B-V$ following the procedure in VandenBerg *et al.* (1990). The dot at $V=14.44$, $B-V=1.06$ represents the M71 horizontal branch.

problems in the amplitude spectra, making the precise determination of a true period difficult. Furthermore it was noted that the B data was of significantly poorer quality than the V data and was consequently excluded from the periodogram analysis.

4.2 Variable H1

H1 (star 81 in Table 2) is in the blue straggler region of the CMD (see Fig. 1). We have identified this star with the star KC-211 from Cudworth (1985) who assigns it a cluster membership probability of only 42% based upon its proper motion. However the V magnitude of this star is close to Cudworth's limiting magnitude, and is in a fairly crowded portion of the field, so we will continue with the following discussion under the assumption that H1 is a cluster member. Figure 5(a) shows the light curve for this star for the first, second, and fourth nights of observations. Figure 5(b) shows similar data for a star (number 385 in Table 2) of similar magnitude and position as H1 for comparison purposes. Figure 5(c) shows the resultant amplitude spectrum from 0 to 50 c/d with a spacing of 0.01 c/d. The highest peak, with an amplitude of 0^m055, at approximately 19.96 c/d, corresponds to a period of 0^d050. There are significant aliasing problems in the data, as can be seen in this figure and other possible periods include 0^d055, 0^d053, and 0^d046. However the best phase diagram is obtained for the period of 0^d050, shown in Fig. 5(d).

Variable H1 appears to be a variable blue straggler of the SX Phe type (Nemec 1989). This is the first such star to be found in the vicinity of a metal-rich globular cluster, although they are known in the metal-poor globular cluster NGC 5466 (Mateo *et al.* 1990) and in ω Cen (Jørgensen 1982; Jørgensen & Hansen 1984; DaCosta & Norris 1988). For a cluster distance modulus of 13.70 ± 0.20 (Richer & Fahlman 1988), the mean V magnitude of 16.252 ± 0.006 leads to an absolute magnitude $\langle M_V\rangle=2.55\pm0.20$. If the star is placed on the period–luminosity relation shown in Fig. 7 of Nemec (1989) one sees that it is most probably a first overtone mode pulsator.

Knowing the absolute magnitude and the pulsation period, the mass of H1 can be derived from the period–mean density relation (see, for example, van Albada & Baker 1971) of which Nemec & Mateo (1991) give the variant

$$\log\frac{\mathscr{M}}{\mathscr{M}_\odot}=2\log\frac{Q_m}{P_m}-0.6M_{\rm bol}-6\log T_e+25.40, \quad (1)$$

where the subscript m refers to the pulsation mode and $M_{\rm bol}$ is the bolometric magnitude. P and ρ are the period and mean density respectively. The pulsation constant Q was

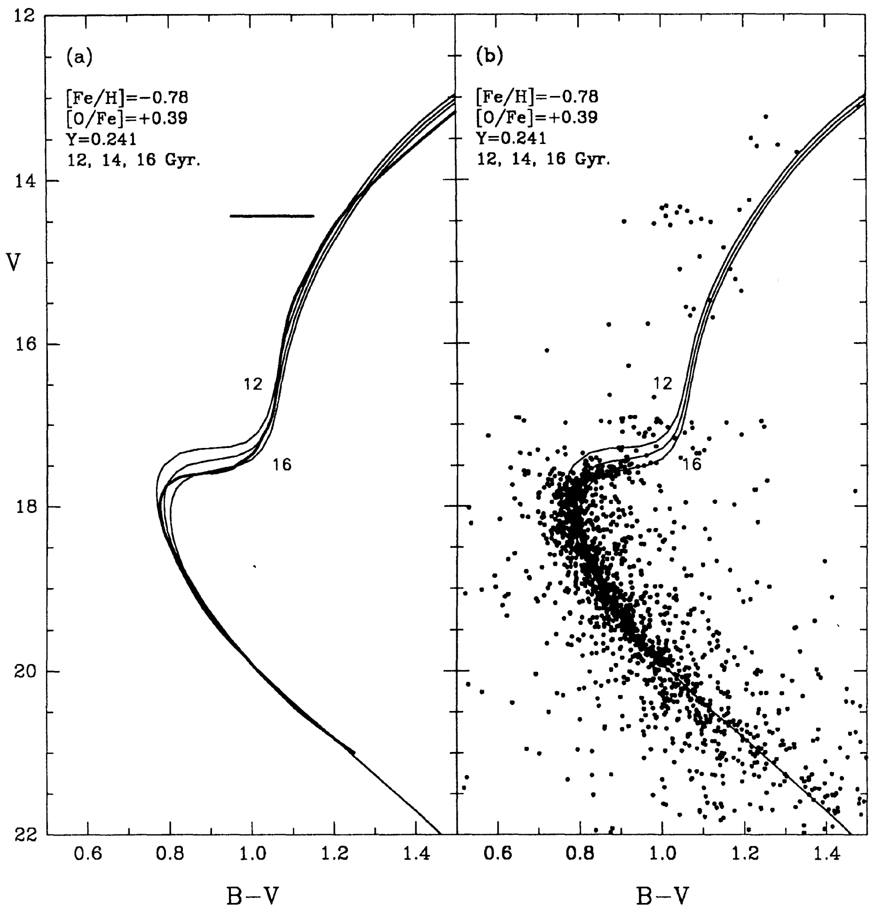

FIG. 4. Comparison of the M71 fiducial with theoretical isochrones by Bergbusch & VandenBerg (1991), and used by Hesser *et al.* (1987) in their study of 47 Tuc. In both panels the isochrones have been shifted using a distance modulus of 13.7 and a reddening of 0.28. An additional shift in $B-V$ of 0.015 was required to match the fiducial. (a) Fits to oxygen enhanced isochrones with an [Fe/H] of -0.78. The 14 and 16 Gyr isochrones provide the best fits. (b) The same isochrones plotted together with our photometry from Fig. 1.

taken to be 0.0333 for the fundamental mode and 0.0252 for the first overtone mode (Petersen & Jørgensen 1972). Errors of 10% in these quantities were assumed. The error of the period was derived by fitting a parabola to 21 points from the amplitude spectrum—the peak point at 19.96 c/d, together with 10 points on either side. Errors in the fitting parameters led to an error of $0^d.0004$ in the position of the peak. Values for the effective temperature (of 7900 ± 400 K) and the bolometric correction (B.C.) ($-0^m.11 \pm 0.05$) were obtained by interpolation of Table 66 of Lang (1986). The errors in the quantities calculated from these tables are "worst case" estimates.

Assuming a first overtone pulsation mode, we derive a mass of

$$\mathscr{M}_{\rm H1} = (0.90 \pm 0.47)\mathscr{M}_\odot$$

where the error in the mass was calculated using standard error propagation techniques. Note that if the star is pulsating in the fundamental mode the following mass results:

$$\mathscr{M}_{\rm H1} = (1.58 \pm 0.83)\mathscr{M}_\odot.$$

The mass we derive for H1 (assuming a first overtone mode of pulsation) is somewhat lower than the mean mass of most SX Phe stars. The derived masses of all known SX Phe variables lie in the range ~ 1.0 to $\sim 1.6\ \mathscr{M}_\odot$ with a mean mass of $\sim 1.2\mathscr{M}_\odot$ (Nemec 1989; Nemec & Mateo 1990). Nemec & Harris (1987) have also computed (via dynamical arguments) the mean mass of all the blue stragglers in NGC 5466 to be $\sim 1.2\mathscr{M}_\odot$. Given the large uncertainty associated with the result, our estimate of the mass of H1 is consistent with the hypothesis that it is an SX Phe star in M71. Note that if a mass of $\sim 1.2\mathscr{M}_\odot$ is adopted for H1, the required distance modulus of the star is 13.9, which is within the allowed uncertainty of the M71 distance modulus.

4.3 Variable H2

H2 (1152 in Table 2) appears on Fig. 1 to be a faint, very blue star, lying approximately $1^m.75$ below the main sequence turnoff point. The light curve for H2 is shown in Fig. 6(a). Figure 6(b) shows the light curve for a comparison star to H2 (star 1215 in Table 2). The initial amplitude spectrum generated for the V data revealed several strong peaks around 17 c/d, five of which gave reasonably good phase diagrams (these were at 16.5303, 16.8503, 17.1803, 17.5103, and 17.8403 c/d). A second amplitude spectrum was obtained using a frequency grid with an interval of 0.01 c/d over a range 10–30 c/d. This is shown in Fig. 6(c) where the effect of the alias frequency of around 1 c/d can also be seen. The strongest peak, with an amplitude of $0^m.053$ and a period of $0^d.0582$ was found to produce the best phase diagram in that it had the least dispersion about a sine curve.

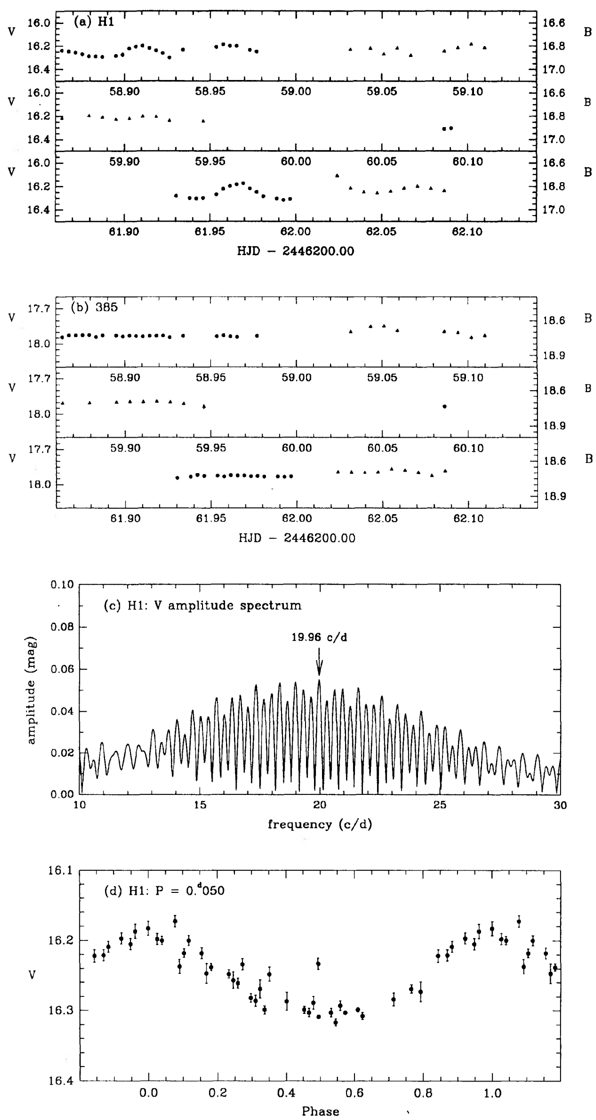

FIG. 5. (a) The light curve for the variable H1. Data for the first, second and fourth nights of observation are plotted in the upper, middle, and lower panels, respectively. (b) A similar plot for star 385 of Table 2, of comparable magnitude, and similar position in the field. In these, and the plots of a similar nature that follow these two, the error bars returned by DAOPHOT have been plotted but are generally smaller than the symbols used to plot the points. (c) An amplitude spectrum generated using the data shown above. The maximum peak of 19.3 c/d is indicated. (d) A phased light curve generated from the data shown above with a period of 0^{d}050. The epoch for the phasing was chosen to be HJD 2446261.96540, the heliocentric Julian Date of the brightest magnitude in the sequence.

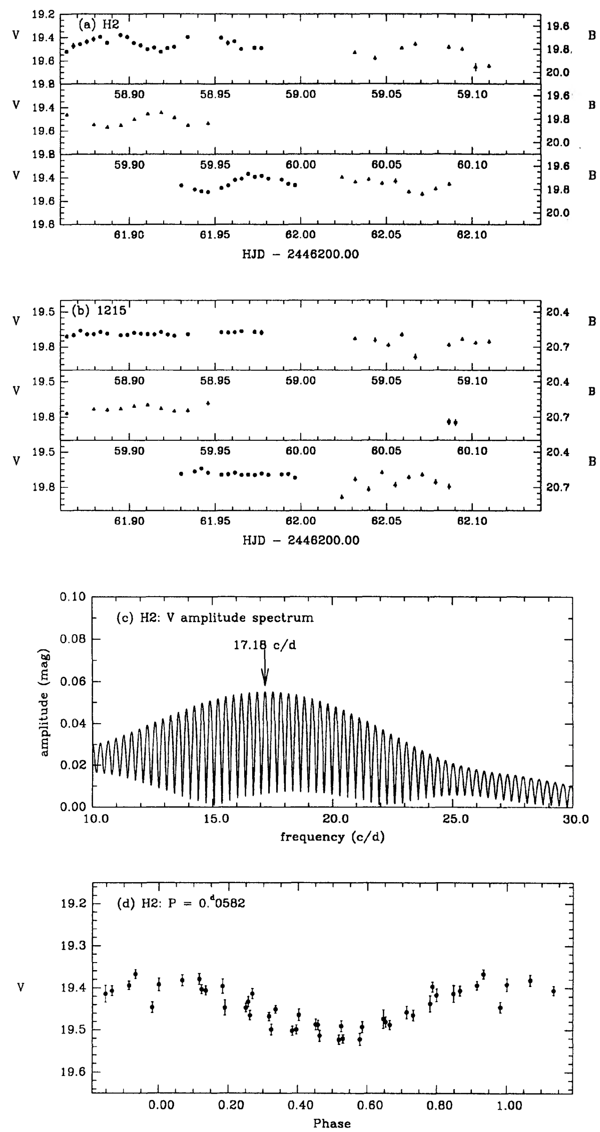

FIG. 6. (a) The light curve for the variable H2. The plot is similar in fashion to Fig. 5(a). (b) A similar plot for star 1215 of Table 2, of comparable magnitude and similar position in the field. (c) An amplitude spectrum generated using the data shown above. (d) A phased light curve generated from the data shown above with a period of 0^{d}0582 corresponding to the frequency of the central (and highest) peak in the amplitude spectrum. The phasing epoch was HJD 2446261.96930.

As seen in Fig. 1, H2 lies blueward of the main sequence, below the turnoff point near to the white dwarf/hot subdwarf region of the CMD (Richer & Fahlman 1988; Drukier *et al.* 1989). The photometry of Richer & Fahlman (1988) verifies the blue color of this star. If this star is indeed a cluster member then its position in the CMD is quite unusual. With such a low luminosity and a period typical of a dwarf Cepheid, it is possible that this is a field star superimposed on the cluster. On the other hand, Kaluzny (1989) has shown the existence of an "extension" of the blue straggler sequence down to the left of the main sequence in the cluster NGC 188. *If* the star H2 found in this study is a member of M71 and is similar to the NGC 188 stars then it may imply an extension of the instability strip down to these low luminosities. We note that the shape of the light curve suggests that it is unlikely to be a W UMa type binary.

4.4 Variable H3

In Fig. 1 the variable H3 (star 865 in Table 2) lies well to the right of the main sequence, suggesting that it may be a field star. The light curve is shown in Fig. 7(a), with a comparison star shown in Fig. 7(b) (star 935 in Table 2). It appears to be more like that of an eclipsing binary star than that of a pulsator. From Fig. 7(a) it can be seen that there is insufficient phase coverage for any accurate periods to be determined. Despite this, an amplitude spectrum was generated from the V data in the manner described above. It showed several peaks in the region 3–8 c/d, the highest being at 5.37 c/d. In an examination of the B data, two peaks of significant amplitude were found at 5.37 and 10.40 c/d. In order to try and increase the phase coverage the two sets of data were then merged by normalizing the B data to the V data. The most noticeable features were peaks at 4.39 and 5.37 c/d. It was found that the latter frequency (a period of $0^{\mathrm{d}}186$) produced the best phase diagram, though there are substantial gaps in the phase coverage.

The shape of the light curve for this star is unusual. If it is a binary star, such as a W UMa type variable, the $0^{\mathrm{d}}186$ period should be doubled to give $0^{\mathrm{d}}372$. However the shape of the light curve is not a good match to other W UMa variables [e.g., the stars NH19 and NH30 in NGC 5466 (Nemec & Harris 1987; Mateo *et al.* 1990)]. Further investigation of this star is required to confirm or refute its variability.

4.5 *Variable H4*

No period analysis could be done on variable H4 (star 333 in Table 2) since it appears that only one cycle has been observed [see Fig. 8(a)]. Figure 8(b) shows the light curve for star 80 (Table 2), included for comparison purposes. The shape of the light curve is strongly suggestive of an eclipsing binary system. If verified this would be of some interest because (excluding W UMa stars) there is only one other eclipsing binary positively identified in a globular cluster. That star is NJL5 in ω Cen, discovered by Niss *et al.* (1978) and confirmed as being a radial velocity member of ω Cen by Jensen & Jørgensen (1985) and Margon & Cannon (1989). However in our case the star H4 seems peculiarly placed on the M71 CMD and radial velocity information would be required to confirm membership for H4.

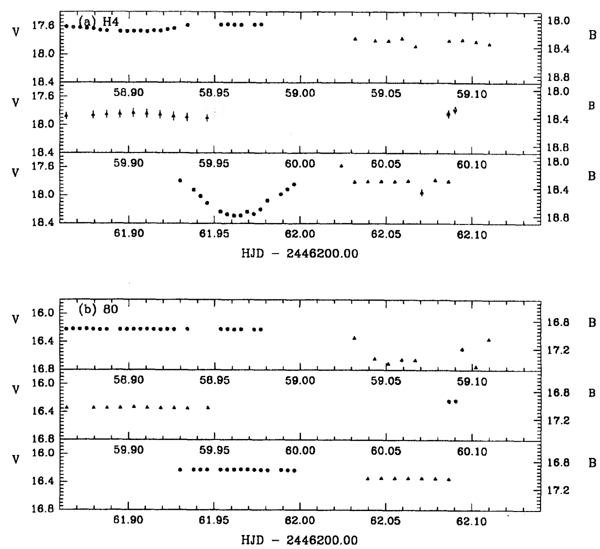

FIG. 8. (a) The light curve for the variable H4. The plot is similar in fashion to Fig. 5(a). (b) A similar plot for star 80 of Table 2 of comparable magnitude and similar position in the field. This star was identified by Cudworth (1985) as KC-371.

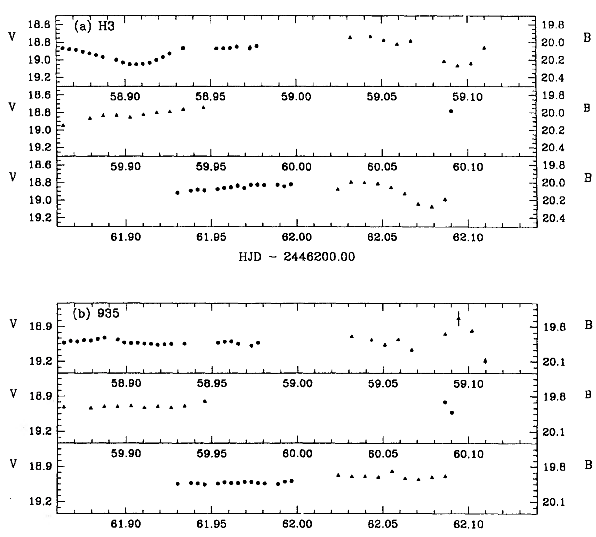

FIG. 7. (a) The light curve for the variable H3. The plot is similar in fashion to Fig. 5(a). (b) A similar plot for star 935 of Table 2, of comparable magnitude and similar position in the field.

5. SUMMARY

Using deep CCD photometry we have constructed a CMD of M71 and compared this to the theoretical isochrones of Bergbusch & VandenBerg (1991). Within the accuracy of our data we find no significant age difference between M71 and 47 Tuc when using the method proposed by VandenBerg *et al.* (1991). We note that this determination is critically dependent on the definition of the fiducial sequence near the main sequence turnoff and extending up the lower red giant branch. This fiducial is not well defined by our photometry. Hence the possibility of a relative age difference between 47 Tuc and M71 remains open. The absolute age of M71 obtained by overlaying the isochrones on the CMD appears to be between 14 and 16 Gyr.

A total of 989 stars in a field of M71 were examined for variability on 75 CCD frames. Of these, only four seem to be variable. Variable seeing, and the lack of sufficiently extensive phase coverage, has certainly affected the ability to detect low amplitude variability. One of the ~10 blue stragglers in the variable search field was found to be variable (H1). Its period and luminosity are consistent with it being an SX Phe type variable, similar to those found in other globular clusters. A second variable (H2) may very well be a field dwarf Cepheid.

Two possible binary stars were also found. The first of these (H3) has a period consistent with it being a W UMa star. These have also been found in the blue straggler region of other clusters—however this star lies to the red side of the main sequence and may also be a field star. The second possible binary lies close to the blue straggler region. Further work is required to confirm the variability of this star.

No main sequence binaries were found in the variable search field, and from the CMD of the larger field there is no evidence of a "binary sequence" $\sim 0^m_.75$ above the main sequence. However it is likely that we do not have a large enough sample to properly address that question. By simply summing the magnitudes of the stars with $V \leqslant 23$ listed in Table 2, we calculate that the total integrated light in the larger survey is $9^m_.03$. On the same basis the integrated magnitude of the variable search field is $10^m_.35$. Harris & Racine (1979) give the integrated absolute magnitude of the cluster as $-5^m_.6$, which together with a distance modulus of 13.70 (Richer & Fahlman 1988) implies that we have sampled 42% and 13% of the cluster light, respectively. Thus there may be, very approximately, ~25 more variables in M71, of which ~7 may be SX Phe stars.

We would like to thank the anonymous referee and Mario Mateo for making some very useful suggestions on the first draft of this paper. P.J.C.H. acknowledges the award of a Graduate Student Fellowship from the University of British Columbia. This research is partially supported by Operating Grants from the Natural Science and Engineering Council of Canada.

REFERENCES

Allen, C., & Martos, M. A. 1988, RMxA, 16, 25
Arp, H., & Hartwick, F. D. A. 1971, ApJ, 167, 499
Bergbusch, P. A., & VandenBerg, D. A. 1991, ApJ (in press)
Bessell, M. S. 1983, PASP, 95, 94
Cohen, J. G. 1980, ApJ, 241, 981
Cudworth, K. M. 1985, AJ, 90, 65
DaCosta, G. S., & Norris, J. 1988, in The Second Conference on Faint Blue Stars, IAU Colloqium No. 95, edited by A. G. D. Philip, D. S. Hayes, & J. W. Liebert (Davis, Schenectady), p. 579
Deeming, T. J. 1975, Ap&SS, 36, 137
Drukier, G. A., Fahlman, G. G., & Richer, H. B. 1989, ApJ, 342, L27
Frogel, J., Persson, S. E., & Cohen, J. 1979, ApJ, 227, 499
Harris, W. E., & Racine, R. 1979, ARA&A, 17, 241
Heasley, J. N., & Christian, C. A. 1991, in Formation and Evolution of Star Clusters, edited by K. Janes (ASP, San Francisco), p. 266
Hesser, J. E., Harris, W. E., VandenBerg, D. A., Allwright, J. W. B., Shott, P., & Stetson, P. B. 1987, PASP, 99, 739 (H87)
Hodder, P. J. C., Nemec, J. M., Richer, H. B., & Fahlman, G. G. 1991, in Formation and Evolution of Star Clusters, edited by K. Janes (ASP, San Francisco), p. 269
Jensen, K. S., & Jørgensen, H. E. 1985, A&AS, 60, 229
Jørgensen, H. E. 1982, A&A, 108, 99
Jørgensen, H. E., & Hansen, L. 1984, A&A, 133, 165
Kaluzny, J. 1990, AcA, 40, 61
Kurtz, D. W. 1985, MNRAS, 213, 773
Lang, K. R. 1986, Astrophysical Formulae—A Compendium for the Physicist and Astrophysicist, 2nd ed. (Springer, New York)
Leep, E. M., Oke, J. B., & Wallerstein, G. 1987, AJ, 92, 338
Liller, M., & Tokarz, S. 1981, AJ, 86, 669
Margon, B., & Cannon, R. D. 1989, Observatory, 109, 82
Mateo, M., Harris, H. C., Nemec, J. M., & Olszewski, E. W. 1990, AJ, 100, 469
Matthews, J. M., & Wehlau, W. H. 1985, PASP, 97, 841
Nemec, J. M. 1989, in The Use of Pulsating Stars in Fundamental Problems of Astronomy, edited by E. G. Schmidt (Cambridge University Press, New York), p. 215
Nemec, J. M., & Harris, H. C. 1987, ApJ, 316, 172
Nemec, J. M., & Mateo, M. 1991, in Confrontation between Stellar Pulsation and Evolution, edited by C. Cacciari and E. Clementini (ASP, San Francisco), p. 64 (to be published)
Niss, B., Jørgensen, H. E., & Lausten, S. 1978, A&AS, 32, 387
Petersen, J. O., & Jørgensen, H. E. 1972, A&A, 17, 367
Richer, H. B., & Fahlman, G. G. 1988, ApJ, 325, 218
Richer, H. B., & Fahlman, G. G. 1989, ApJ, 339, 178
Sarajedini, A., & Demarque, P. 1990, ApJ, 365, 219
Sawyer Hogg, H. 1973, Publ. DDO, 3, No. 6
Shara, M. M., Kaluzny, J., & Potter, M. 1988, ApJ, 328, 594
Stetson, P. B. 1987, PASP, 99, 191
van Albada, T. S., & Baker, N. 1971, ApJ, 169, 311
VandenBerg, D. A., Bolte, M., & Stetson, P. B. 1990, AJ, 100, 445
VandenBerg, D. A., & Stetson, P. B. 1991, AJ, 102, 1043
Zinn, R. 1985, ApJ, 293, 424